SEISMIC EVALUATION OF R/C FRAMED BUILDING USING SHEAR FAILURE MODEL

A thesis
Submitted by

Avadhoot Bhosale
(210CE2029)

In partial fulfillment of the requirements
for the award of the degree of

Master of Technology
In
Civil Engineering
(Structural Engineering)

Under The Guidance of
Dr. Pradip Sarkar

Department of Civil Engineering
National Institute of Technology Rourkela
Orissa -769008, India
May 2012

NATIONAL INSTITUTE OF TECHNOLOGY
ROURKELA, ORISSA -769008, INDIA

This is to certify that the thesis entitled, "**SEISMIC EVALUATION OF R/C FRAMED BUILDING USING SHEAR FAILURE MODEL**" submitted by **Avadhoot Bhosale** in partial fulfillment of the requirement for the award of **Master of Technology** degree in **Civil Engineering** with specialization in **Structural Engineering** at the National Institute of Technology Rourkela is an authentic work carried out by his under my supervision and guidance. To the best of my knowledge, the matter embodied in the thesis has not been submitted to any other University/Institute for the award of any degree or diploma.

Research Guide

Place: Rourkela
Date:

Dr. Pradip Sarkar
Associate Professor
Department of Civil Engineering
NIT Rourkela

ACKNOWLEDGEMENTS

First and foremost, praise and thanks goes to my God for the blessing that has bestowed upon me in all my endeavors.

I am deeply indebted to **Dr. Pradip Sarkar,** Associate Professor of Structural Engineering Division, my advisor and guide, for the motivation, guidance, tutelage and patience throughout the research work. I appreciate his broad range of expertise and attention to detail, as well as the constant encouragement he has given me over the years. There is no need to mention that a big part of this thesis is the result of joint work with him, without which the completion of the work would have been impossible.

I am grateful to **Prof. N Roy**, Head, Department of Civil Engineering for his valuable suggestions during the synopsis meeting and necessary facilities for the research work.

I extend my sincere thanks to **Dr. Robin Davis P** the faculty members of Structural Engineering Division for their helpful comments and encouragement for this work.

I am grateful for friendly atmosphere of the Structural Engineering Division and all kind and helpful professors that I have met during my course.

I would like thank my parents and sister. Without their love, patience and support, I could not have completed this work.

Finally, I wish to thank many friends for the encouragement during these difficult years, especially, **Snehash, Bijali, Kirti, Hemanth, Santosh, Reddy, Malli, Sukumar.**

Avadhoot Bhosale

ABSTRACT

KEYWORDS: shear hinges, shear strength, shear displacement, nonlinear static pushover analysis, hinge property, reinforced concrete.

Prediction of nonlinear shear hinge parameters in RC members is difficult because it involves a number of parameters like shear capacity, shear displacement, shear stiffness. As shear failure are brittle in nature, designer must ensure that shear failure can never occur. Designer has to design the sections such that flexural failure (ductile mode of failure) precedes the shear failure. Also design code does not permit shear failure. However, past earthquakes reveal that majority of the reinforced concrete (RC) structures failed due to shear. Indian construction practice does not guaranty safety against shear. Therefore accurate modelling of shear failure is almost certain for seismic evaluation of RC framed building.

A thorough literature review does not reveal any information about the nonlinear modelling of RC sections in Shear. The current industry practice is to do nonlinear analysis for flexure only. Therefore, the primary objective of the present work is to develop nonlinear force-deformation model for reinforced concrete section for shear and demonstrate the importance of modelling shear hinge in seismic evaluation of RC framed building. From the existing literature it is found that equations given in Indian Standard IS-456: 2000 and American Standard ACI-318: 2008 represent good estimate of ultimate strength. However, FEMA-356 recommends ignoring concrete contribution in shear strength calculation for ductile beam under earthquake loading. No clarity is found regarding yield strength from the literature. Priestley et al. (1996) is reported to be most effective for calculating shear displacement at

yield whereas model proposed by Park and Paulay (1975) is most effective in predicting the ultimate shear displacements for beams and columns. Combining these models shear hinge properties can be calculated.

To demonstrate the importance of modelling shear hinges, an existing RC framed building is selected. Two building models, one with shear hinge and other without shear hinges, are analysed using nonlinear static (pushover) analysis.

This study found that modelling shear hinges is necessary to correctly evaluate strength and ductility of the building. When analysis ignores shear failure model it overestimates the base shear and roof displacement capacity of the building. The results obtained here show that the presence of shear hinge can correctly reveal the non-ductile failure mode of the building.

TABLE OF CONTENTS

Title **Page No.**

Title **Page No**

LIST OF TABLES

Title **Page No**

LIST OF FIGURES

Title **Page No**

ABBREVIATIONS

3D	Three Dimensions
ACI	American Concrete Institute
ADRS	Acceleration-Displacement Response Spectrum
ATC	Applied Technology Council
BS	British Standard
CEB	Comité Euro-Internacional du Béton
CM	Center of Mass
CP	Collapse Prevention
CR	Center of Rigidity
CS	Centre of Stiffness
CSA	Canadian Standards Association
CSM	Capacity Spectrum Method
DCM	Displacement Coefficient Method
DL	Dead load
EL	Earthquake load
FEMA	Federal Emergency Management Agency
IO	Intermediate Occupancy
IS	Indian Standard
LL	Live Load
LS	Life Safety
MPa	Mega Pascal

PCM	Pulse Code Modulation
PGA	Peak Ground Acceleration
Push X	Pushover analysis in X directions
Push Y	Pushover analysis in Y directions
RC	Reinforced Concrete
SDOF	Single Degree of Freedom
SR_A	Spectral Reduction factor in constant accelerations region
SR_v	Spectral Reduction factor in constant velocity region
T	Time period
WL	Wind Load

NOTATIONS

English

l_p	Equivalent length of plastic hinge
A	Shear span
a/d	Shear span to depth ratio
A_g	Gross cross sectional area of concrete
A_{st}	Area of transverse reinforcement
A_{sv}	Area of shear reinforcement
b	Width of member
d	Effective depth of member
D	Total depth of member
d_b	Diameter of longitudinal bar
d_x	Element length of member
E_c	Modulus of elasticity of concrete
EI	Flexural rigidity
E_s	Modulus of elasticity of steel
$f_c^{'}$	Cylindrical compressive strength of concrete
f_{ck}	Characteristic compressive strength of concrete cube
F_i	Lateral force at each story
f_y	Yield stress of the longitudinal reinforcement
f_{yh}	Grade of the stirrup reinforcement
G	Shear modulus
I	Moment of area of section

L	Length of member
Mu	Ultimate moment capacity
M_y	Yield moment capacity
P_t	Percentage of steel
S_a/g	Average response acceleration coefficient
T	Time period
T_{eq}	The equivalent period
T_i	Initial period of vibration of nonlinear system
V_B	Base shear
V_c	Shear strength of concrete
V_p	Shear carried by axial load
V_s	Shear strength of steel
V_u	Ultimate shear strength of concrete
V_y	Yield shear strength of concrete
W	Seismic weight of the building
W_i	Seismic weight of floor i
Z	Seismic Zone factor

Greek

Δ	Roof displacement
α	Angle between inclined stirrups
β_{eq}	Equivalent damping ratio
γ	Shear strain

γ_m	Partial safety factor
δ	Shear displacement
δ_t	Target displacement
θ_p	Plastic rotation
θ_u	Ultimate rotation
θ_y	Yield rotation
μ	Displacement ductility ratio
ρ	Longitudinal reinforcement ratio
τ_c	Design shear strength of concrete
τ_v	Nominal shear stress
φ	Curvature
ω	Frequency

CHAPTER 1

INTRODUCTION

1.1. OVERVIEW

The problem of shear is not yet fully understood due to involvement of number of parameters. In earthquake resistance structure heavy emphasis is placed on ductility. Hence designer must ensure that shear failure can never occur as it is a brittle mode of failure. Designer has to design the sections such that flexural failure (ductile mode of failure) antedates the shear failure. Also, shear design is major important factor in concrete structure since strength of concrete in tension is lower than its strength in compressions. However, past earthquakes reveal that majority of the reinforced concrete (RC) structures failed due to shear. Indian construction practice does not guaranty safety against shear.

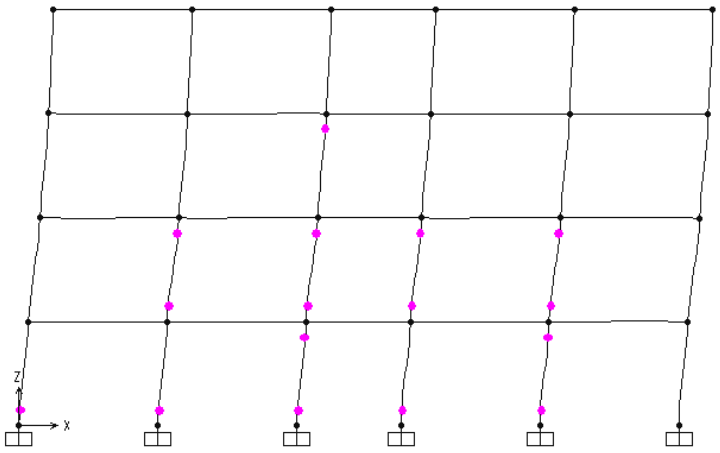

Fig. 1.1: Deformed shape of a nonlinear building model under lateral load

Fig. 1.1 represents deformed shape of a building model under lateral load. Failure through formation of hinges in the columns is also shown in this figure. A nonlinear

analysis like this can predict the failure mode, maximum force and deformation capacity of the structure. But to do an accurate analysis nonlinear modelling of frame sections for flexure and shear is very important.

However, the nonlinear modelling of RC sections in shear is not well understood. A thorough literature review does not reveal any information about the nonlinear modelling of RC sections in Shear. The current industry practice is to do nonlinear analysis for flexure only.

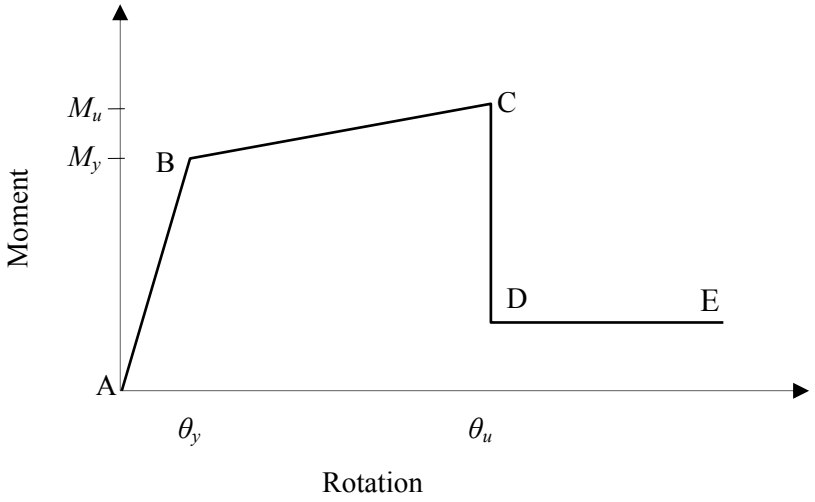

Fig.1.2: Nonlinear models for Moment *v/s* Rotations

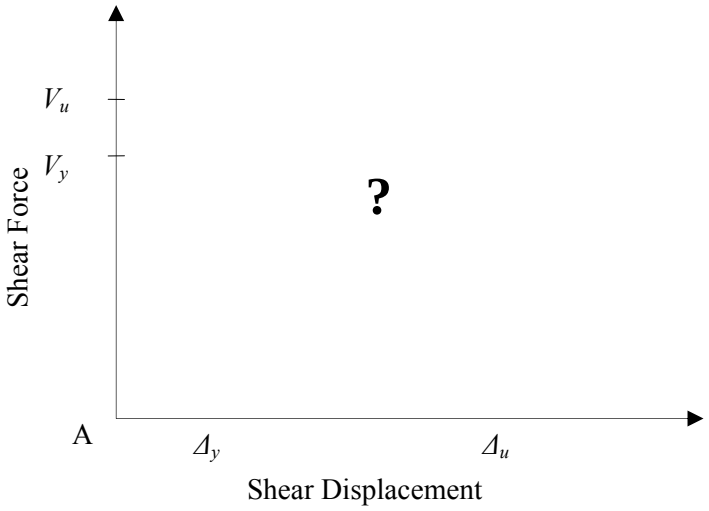

Fig.1.3: Shear force v/s Shear Displacement

Fig. 1.2 presents a typical nonlinear moment rotation curve for RC member. Alternative methods are available in literature to calculate the important points required to define the nonlinear moment rotation curve for any section. In the conventional analysis the sections are generally considered to be elastic in shear although this not true. Therefore, the primary objective of the present work is to develop nonlinear force-deformation model for RC rectangular section for shear (Fig. 1.3). Also it is important to check how nonlinear modelling of shear alters the seismic behaviour of RC framed building.

1.2. LITERATURE REVIEW

An extensive literature review is carried out on the three subjects: (a) Estimation of shear strength of RC section, (b) estimation of shear deformation capacity of RC section and (c) pushover analysis of RC framed buildings. A number of literatures are found on the estimation of shear strength for RC sections with and without web reinforcement. Majority of the previous works on shear strength estimations are based on experimental study. However, there is only one published literature found on the estimation of shear displacement capacity of RC section. There is no literature available that demonstrate the pushover analysis of framed building considering shear failure. Following section presents a brief report of the literature review carried out on the above mentioned subjects as part of this project.

Ghaffar *et. al*. (2010) verified the applications of shear strength equations available in literatures through experimental work. An extensive experimental study was carried out on rectangular reinforced concrete (RC) beams without web reinforcement. By considering three parameters, percentage of tension steel (P_t), compressive strength (f_{ck}) of concrete, and shear span to depth

ratio (*a/d*), new equations are developed for the shear strength estimation. Experimental results of the study show that the concrete shear capacity ranges from $1.7\sqrt{f_c'}$ to $1.8\sqrt{f_c'}$ before any cracking is observed. It shows that contribution of f_c' is about 80 to 90% of the total shear before any cracking which is against the Kani (1979). By considering divorcing point this study developed new equations for predictions of Cracking shear capacity and Ultimate shear capacity. Beam design may be economical if shear capacity supplied by new developed equations are kept in view.

Xu *et*. *al*. (2005) presented shear capability of reinforced concrete beams without stirrups using a fracture mechanics approach. The new analytical formula is developed to shows the contributions of the reinforcement ratio (ρ), shear span to depth ratio (a/d), concrete quality to shear strength and the size effect in shear fracture. Finally from this new formula, shear bearing capability of reinforced concrete beam without stirrups evaluated and compared to that calculated by using Gastebled and May (1998) model, the ACI 318: 1989 Code and CEB-FIP Model Code (1990) respectively. It is further confirmed that fracture mechanics can be applied to know both the mode II fracture toughness KIIc and mode II fracture energy GIIF of concrete materials capability of reinforced concrete beams without stirrups to the assessment of shear bearing important to perform more pure mode II fracture tests for various concrete materials and also provides knowledge to develop analytical formula for shear fracture problems in reinforced concrete members.

Karayannis *et*. *al*. (2005) performed experimental investigations on shear capacity of RC rectangular beam with continuous spiral transverse reinforcement under monotonic loading. Three specimens consist of beam with common stirrups, spiral transversal reinforcement and spiral transversal reinforcement with favourably inclined leg with shear span ratio 2.67

constructed. Based on experimental results and the behavioural curve of tested beams they found that the specimens with continuous spiral reinforcements demonstrated 15% and 17% respectively higher shear strength than the beam with closed stirrups. Beam with spiral reinforcements with favourably inclined legs exhibited enhanced performance and rather ductile response whereas other beam shows brittle shear failure.

Chowdhury (2007) developed a suitable hysteretic model that would predict the lateral deformation behaviour of lightly reinforced or shear-critical columns subjected to gravity and seismic load. Several tests on reinforced concrete columns under lateral loads have shown that the total drift stems from deformations owing to flexure, reinforcement slip, and shear. Existing analytical and experimental research on lightly reinforced columns is examined. This information is used for modify to ultimately develop a suitable overall hysteretic model that would accurately predict the lateral response of this class of columns with a limited computational effort. The behaviour of a column is classified into one of five categories based on a comparison of the shear, yield and flexural strengths. Overall the model did a reasonable job of simulating the load deformation relationships of shear-critical columns and provides a suitable platform to analyze older reinforced concrete buildings with a view to determining the amount of remediation necessary for satisfactory seismic performance.

Sezen and Setzler (2008) focused on modelling the behaviour of reinforced concrete columns subjected to lateral loads. Shear failure in columns initially dominated by flexural response is considered through the use of a shear capacity model. The proposed model was tested on 37 columns from various experimental studies. In general, the model predicted the lateral deformation response envelope reasonably well. The focus of this research was the creation of a model that can predict the monotonic lateral force displacement relationship for reinforced

concrete columns subjected to lateral loading. The research concentrated on lightly reinforced columns that experience flexure-shear failures. However, the model can be applied to columns with any ratio of shear and flexural strengths. Therefore, it is applicable to columns that experience shear, flexure, or flexure-shear failures.

Ahmad *et. al*. (2009) presented statistical model for the prediction of shear strength of high strength reinforced concrete (HSRC) beams. By comparing the actual and predicted values of shear strength of beams it shows that the proposed equation is conservatives for various longitudinal reinforcement ratios (ρ). It also compared the predicted values of shear strength to the values proposed by ACI, Russo et al. (2004), and Bazant et al. (1984). Bazant et al. (1984) is found to be un-conservative in estimating the shear stress for the HSRC beams without web reinforcement. The Russo et al. (2004) is more conservative as it underestimates the shear strength of the HSRC beams without web reinforcement. The ACI-318 equation for shear strength of HSRC beams gives some reasonable values when compared with the actual and predicted values. The Russo et al. (2004) on the other hand, is un-conservative for shear strength of HSRC beams with web reinforcement.

Wafa *et. al*. (1994) carried out experiment investigations on shear behaviour of reinforced high strength concrete beam without shear reinforcement. 18 rectangular beams are tested in combined shear and flexure and compared the experimental shear capacities with shear capacities predicted by different empirical equations. Two empirical equations have been proposed to better predict the shear capacity of reinforced high strength concrete beams without stirrups. The study concluded that beam of low reinforcement ratios fail in flexure irrespective of their *a/d* values. Modifications in the ACI code equations (2008) and Zsutty's equations

(1968,1971) have been proposed to predict the shear capacity of reinforced high strength concrete beam without stirrups.

Paczkowski and Nowak (2008) reviewed the available data base and shear model for reinforced concrete beams without shear reinforcement and select the most efficient model for design code for concrete structure. The relationship between shear capacity and parameters such as width and depth of beam, longitudinal reinforcement ratio and compressive strength of concrete has been established by using test results.

Zakaria *et. al*. (2009) present experimental investigations to clarify shear cracking behaviour of reinforced concrete beams. Test results show that shear reinforcement characteristics, longitudinal reinforcement ratios, the distance of shear crack from the crack tip and the intersections with nearest reinforcement's ratio play critical role in controlling diagonal crack spacing and openings. This research concluded that shear cracks width increases proportionally with both the strain of shear reinforcements and the spacing between the shear cracks. This implies that the stirrups strain and diagonal crack spacing are main factors on shear crack displacements.

Rao and Injaganeri (2011) performed nonlinear analysis for developing the refined design models for both the cracking and ultimate shear strength of reinforced concrete beam without web reinforcement. The proposed models are functions of cylindrical compressive strength ($f_c^{'}$), longitudinal reinforcement ratio (ρ) and effective depth (d). The proposed models have been validated with the existing popular model as well as with the design code provisions. The study concluded that proposed model to predict the ultimate shear strength is simple and predicts shear strength of RC beams with fair degree of accuracy on the deep, short and normal beams.

Angelakos (1999) investigated the influence of concrete strength and main longitudinal reinforcement ratio on the shear capacity of large, lightly reinforced concrete members with and without transverse reinforcement. In addition, the test results were used to assess the performance of the North American code provisions, AC1 318-95 and CSA A23 -3-94 (General Method). It is found that the general method of CSA A23 -3-94 yielded much better predictions than the AC1 approach. The five beam specimens constructed with 1% longitudinal reinforcement without stirrups and several concrete strengths had essentially the same ultimate shear capacity. The implementation of high-strength concrete proved to be beneficial only when transverse reinforcement was utilized.

Patwardhan (2005) presented lateral load- shear displacement relationship. By using available experimental data they evaluated existing available model. The modified compression filed theory is very complicated to implement but results are to be very accurate. In this study through investigations of modified compression filed theory analyses performed. By comparing proposed model with the predictions obtained from existing models and experimental data. The study concluded that in predicting lateral load – shear displacement relations the proposed model is simple and give accurate results.

Kadid and Boumrkik (2008) evaluated the performance of framed buildings under earthquakes with the help of a nonlinear static pushover analysis. Three framed buildings were analyzed with 5, 8 and 12 stories respectively and results obtained from this study show that under seismic loads, properly designed frames will perform well. This study based on flexural hinge model concludes that the pushover analysis is relatively simple method to explore the nonlinear behaviour of buildings. By the intersection of the demand and capacity curves and the distribution of hinges in the beams and the columns, the behaviour of properly detailed

reinforced concrete frame building is adequately indicated. Most of the hinges are formed in the beams and few in the columns with limited damage.

Inel and Ozmen (2006) considered four and seven-story buildings to investigate the possible differences in the results of pushover analysis due to user defined nonlinear component properties for flexure. Pushover analysis is carried out assuming effective parameters like plastic hinge length and transverse reinforcement spacing for user-defined hinge properties. Plastic hinge length and transverse reinforcement spacing found to have no influence on the base shear capacity but they have considerable effects on the displacement capacity of the frames. Displacement capacity improves by increasing the amount of transverse reinforcement. From this study they can observe that displacement capacity of the frames is greatly influenced by plastic hinge length (L_p). Comparisons show that there is a variation of about 30% in displacement capacities due to plastic hinge length. Modern code compliant buildings may yield a reasonable capacity curve for the default-hinge model but this model is not suitable for other type of buildings. Also observations clearly show that in reflecting nonlinear behaviour compatible with the element properties the user-defined hinge model is better than the default-hinge model.

1.3. OBJECTIVES

Based on the literature review presented above salient objectives of the present study are defined as follows:

i) To develop nonlinear modelling parameters of rectangular RC members with transverse reinforcement in shear.

ii) To carry out a seismic evaluation case study of a RC framed building considering nonlinearity in shear as well as flexure using the developed modelling parameters.

1.4. SCOPE OF THE STUDY

i) Only rectangular sections are considered for the present study.

ii) Spiral web reinforcement is kept outside the scope of the present study.

iii) Stress-strain relation for reinforcing steel is taken from the IS 456:2000.

1.5. METHODOLOGY

i) Carry-out detailed literature review on behaviour of shear in RC rectangular sections to determine nonlinear modelling parameters (yield and ultimate shear strength and associated displacement).

ii) Carry out a case study of seismic evaluation of a RC building considering nonlinearity in shear as developed in the present study.

1.6. ORGANIZATION OF THESIS

This introductory chapter (Chapter 1) presents the background and motivation behind this study followed by a brief report on the literature survey. The objectives and scope of the proposed research work are presented in this chapter.

Chapter 2 reviews major international design codes with regard to the shear provision. This includes Indian Standard IS 456: 2000, British standard BS 8110: 1997 (Part 1), American Standard ACI 318: 2008 and FEMA 356: 2000.

Chapter 3 includes the discussions of existing models for shear capacity with and without web reinforcement. Alternate shear capacity calculation procedures for structural member as per published literature are illustrated in this chapter.

Chapter 4 presents the existing models available for shear displacement at yield and ultimate failure point. Existing procedures of shear displacement calculation for RC sections are discussed in this chapter.

Chapter 5 presents the details of the selected building for the case study, computational modelling details of selected buildings. It also describes in detail the modelling of nonlinear force deformations behaviour for flexural and shear hinges.

Chapter 6 presents and discusses the results obtained from nonlinear pushover analysis of the selected building considering (and ignoring) shear hinge model.

Finally, in Chapter 7, the summary and conclusions are presented. The scope for future work is also discussed.

CHAPTER 2

REVIEW OF CODE PROVISIONS

2.1. OVERVIEW

This chapter reviews major international design codes with regard to the shear provision in RC section. This includes Indian Standard IS 456: 2000, British standard BS 8110: 1997 (Part 1), American Standard ACI 318: 2008 and FEMA 356: 2000. The shear capacity of a section is the maximum amount of shear the beam can withstand before failure. In a RC member without shear reinforcement, shear force generally resisted by:

i) Shear resistance V_{cz} of the uncracked portion of concrete.

ii) Vertical component V_{ay} of the 'interface shear' (*aggregate interlock*) force V_a.

iii) Dowel force V_d in the tension reinforcement (due to dowel action).

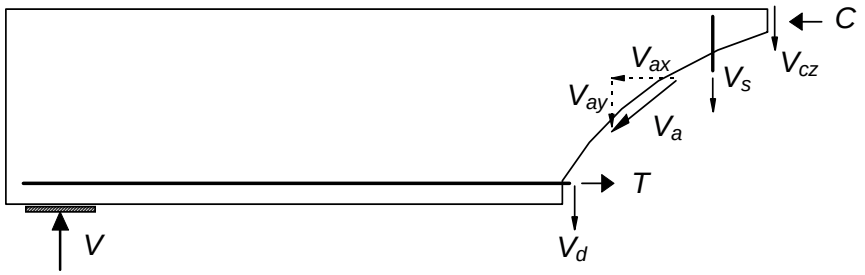

Fig.2.1. Shear Transfer Mechanism

Member with shear reinforcement, shear force is mainly carried by uncracked portion of concrete (V_{cz}) and transverse reinforcement (V_s). Shear carried by aggregate interlock (V_a) and dowel force in the tension reinforcement (V_d) are very small hence their effects are considered negligible.

International design codes except British Standard recommend procedures to calculate shear strength of rectangular and circular RC sections with transverse reinforcement. However, all the design codes are silent about the maximum shear displacement capacity of RC sections. Shear strength estimation procedures as per few major international codes are discussed as follows.

2.2. INDIAN STANDARD (IS 456: 2000)

Indian standard IS 456: 2000 as per Clause 40.1, specify the nominal shear stress by following equations.

$$\tau_v = \frac{V_u}{bd} \qquad (2.1)$$

Shear carried by concrete is given by

$$V_u = \delta\ \tau_c\, bd \qquad (2.2)$$

$$Where\ \ \delta = 1 + \frac{3P_u}{A_g\ f_{ck}} \le 1.5\ and\ \tau_c = \frac{0.85\sqrt{0.8\, f_{ck}}\left(\sqrt{1+5\beta}\ -1\right)}{6\beta}$$

$$Here\ \beta = \frac{0.116\, f_{ck} bd}{100 A_{st}} \ge 1.0$$

As per clause *40.2.2*, for member subjected to axial compression P_u **,** the design shear strength of concrete, given in Table 19 shall be multiplied by the following factor :

$$\delta = 1 + \frac{3P_u}{A_g\, f_{ck}} \le 1.5 \qquad (2.3)$$

The design shear strength of concrete *(* τ_c *)* in beam without shear reinforcements is given in Table 19. τ_c depend upon percentage of steel p_t which is given by

$$p_t = \frac{100Ast}{bd} \qquad (2.4)$$

If τ_v exceeds τ_c given in Table *19* , Shear reinforcement shall be provided in any of the following forms:

- Vertical stirrups
- Bent-up bars along with stirrups
- Inclined stirrups

Contribution of web reinforcement in shear strength given in *IS-456: 2000* represent ultimate strength of the stirrups given by

$$V_s = 0.87 f_y A_{sv} \frac{d}{s_v} \quad \textit{for vertical stirrups} \qquad (2.5)$$

$$V_s = 0.87 f_y A_{sv} \sin\alpha \quad \textit{for bent up bars} \qquad (2.5.a)$$

$$V_s = 0.87 f_y A_{sv} \frac{d}{s_v}(\sin\alpha + \cos\alpha) \quad \textit{for inclined stirrups} \qquad (2.5.b)$$

2.3. BRITISH STANDARD (BS 8110: 1997, PART 1)

British standard BS 8110: PART 1 as per clause *3.4.5.2*, specify the nominal shear stress by following equations.

$$v = \frac{V}{b_v d} \qquad (2.6)$$

Where b_v is the breadth of the section. For a flanged beam width is taken as the width of the rib below the flange. V is the design shear force due to ultimate loads and d is the effective depth. The code gives in Table *3.9* the design concrete shear stress v_c which is used to determine the shear capacity of the concrete alone. Values of v_c depend on the

percentage of steel in the member, the depth and the concrete grade. The design concrete shear stress is given by

$$V_c = \left[\frac{0.79}{\gamma_m}\right] \times \left[\frac{100A_s}{bd}\right]^{\frac{1}{3}} \times \left[\frac{400}{d}\right]^{\frac{1}{4}} \times \left[\frac{f_{cu}}{25}\right]^{\frac{1}{3}} \text{ for } \frac{a}{d} > 2 \qquad (2.7)$$

where $\frac{100A_s}{bd} \le 3, \frac{400}{d} \ge 1, \gamma_m = 1.25 \,\&\, f_{cu} \le 40MPa$.

2.4. AMERICAN CONCRETE INSTITUTE (ACI318: 2008)

ACI 318: 2008, specify that the shear strength is based on an average shear stress on the full effective cross section $b_w\, d$. For a member without shear reinforcement, shear is assumed to be carried by the concrete web and member with shear reinforcement, a portion of the shear strength is assumed to be provided by the concrete and the remainder by the shear reinforcement.

As per clause *11.2*,

$$V_y = V_c + V_s \qquad (2.8)$$

$$V_c = \delta \times \left(0.17\sqrt{f_c^{'}}\right) \times bd \quad \left(\text{where, } \delta = 1 + \frac{P_u}{14A_g}\right) \qquad (2.9)$$

$$V_s = \frac{A_{sv} \times f_{yh} \times d}{s_v} \quad \textit{for vertical stirrups} \qquad (2.10)$$

$$V_s = \frac{A_{sv} \times f_{yh} \times d}{s_v}(\sin\alpha + \cos\alpha) \ \textit{for inclined stirrups} \qquad (2.10.a)$$

2.5. FEDERAL EMERGENCY MANAGEMENT AGENCY (FEMA 356)

FEMA-*356* does not consider contribution of concrete in shear strength calculation for beam under earthquake loading. FEMA-*356* consider ultimate shear strength carried by

the web reinforcement (= strength of the beam) as *1.05* times the yield strength. But there is no engineering background for this consideration.

2.6. SUMMARY

In this chapter the provisions for shear capacity in different international codes are explained. All the major international codes are using similar function to calculate shear capacity. However, the prescribed values of the coefficients differ from code to code.

CHAPTER 3

SHEAR CAPACITY MODEL

3.1. SHEAR CAPACITY

The shear capacity of a section is the maximum amount of shear the section can withstand before failure. Based on theoretical concept and experimental data researchers developed many equations to predict shear capacity but no unique solutions are available. Several equations are available to determine shear capacity of RC section, *i.e*., ACI 318:2005 equations, Zsutty's equation (1968,1971) and Kim and White equation (1991) etc. To verify the applicability of these equations experimental study was carried out by several researchers on rectangular RC beam with and without web reinforcement. Three parameters: cylindrical compressive strength ($f_c^{'}$), longitudinal reinforcement ratio (ρ) and shear span-to-depth ratio (a/d) are considered for developing equations for estimating shear strength of RC section without web reinforcement.

3.1.1. Factors affecting shear capacity of beam

There are several parameters that affect the shear capacity of RC sections without web reinforcement. Following is a list of important parameters that can influence shear capacity of RC section considerably:

- Shear span to depth ratio *(a/d)*
- Tension steel ratio *(ρ)*
- Compressive strength of Concrete *(fc)*

- Size of coarse aggregate
- Density of concrete
- Size of beam
- Tensile strength of concrete
- Support conditions
- Clear span to depth ratio *(L/d)*
- Number of layers of tension reinforcement
- Grade of tension reinforcement
- End anchorage of tension reinforcement.

3.1.2. Shear capacity near support

BS-8110:1997 Part 1 (clause 3.4.5.8) states that shear failure in beam sections without shear reinforcement normally occurs at about *30°* to the horizontal. Shear capacity increases if the angle is steeper due to the load causing shear or because the section where the shear is to be checked is close to the support.

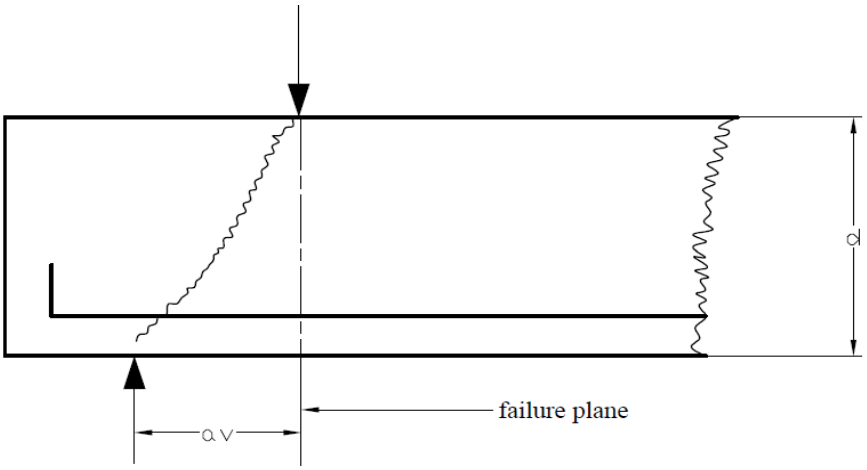

Fig.3.1. Shear capacity near support

The increase is because the concrete in diagonal compression resists shear (Fig. 3.1). The shear span ratio a_v/d is small in this case. The design concrete shear can be increased from V_c as determined above to $2V_cd/a_v$. Where a_v = length of that part of a member traversed by a shear plane.

3.1.3. Maximum design shear capacity

BS8110: 1997, Part 1, clauses 3.4.52 and 3.4.58 states that

$$\text{Nominal shear stress } v = \frac{V}{bd} \leq 0.8\text{fcu}^{1/2} \text{ or } 5 \text{ N/mm}^2$$

even if the beam is reinforced to resist shear. This upper limit prevents failure of the concrete in diagonal compression. If v is exceeded the beam must be made larger.

3.2. MODES OF FAILURE IN SHEAR

Modes of shear failure for beam without web reinforcement depend on the shear span. Shear failure is generally classified based on shear span into three types as follows:

i) Diagonal tension failure ($a > 2d$)

ii) Diagonal compression failure ($d \leq a \leq 2d$)

iii) Splitting or true shear failure ($a < d$)

3.3. SHEAR CAPACITY EQUATIONS

A number of equations for estimating shear capacity of beam section are available in literature. This section compiles these equations in two subheadings: (a) beams without web reinforcement and (b) beams with web reinforcement

3.3.1. Beam without web reinforcement

3.3.1.1. Zsutty (1968, 1971)

Zsutty (1968, 1971) developed two different equations for different *a/d* by combining the techniques of dimensional and statistical regression analysis.

$$v_u = 2.3\left(f_c' \times \rho \times \frac{d}{a}\right)^{\frac{1}{3}} MPa \qquad for\ \frac{a}{d} \geq 2.5 \qquad (3.1)$$

$$v_u = 2.3\left(f_c' \times \rho \times \frac{d}{a}\right)^{\frac{1}{3}} \times \left(2.5\frac{d}{a}\right) MPa \quad for\ \frac{a}{d} < 2.5 \qquad (3.1.a)$$

However Zsutty fails to impose maximum and minimum limits on the variables as ACI placed a limit of $3.5\sqrt{fc'}$ and Placas and Regan (1971) placed a limit of $12(fc')^{1/3}$ on the maximum estimated value of ultimate shear.

3.3.1.2. Mphonde and Frantz (1984)

Mphonde and Frantz (1984) developed an equation for shear strength of rectangular reinforced beams using regression analysis. This equation has a very limited application and is only valid for *a/d* = 3.6.

$$v_u = 0.336\left(f_c'\right)^{\frac{1}{3}} + 0.49 \quad MPa \qquad (3.2)$$

f_c' is considered in this equation and contribution of steel ratio and shear span to depth ratio are altogether ignored.

3.3.1.3. Bazant and Kim (1984)

Bazant and Kim (1984) developed the following equations for shear capacity considering maximum aggregate size in concrete:

$$v_u = \left[\frac{10\sqrt[3]{\rho}}{1+\frac{d}{25\times ag}}\right]\times\left[0.083\sqrt{f_c'}+20.69\sqrt{\frac{\rho}{(a/d)^5}}\right] MPa \qquad (3.3)$$

Where *ag* = Max. aggregate size.

In this equation five parameters (*fc′, ρ, d/a, d* and *ag*) are correlated with ultimate shear strength of rectangular beams, especially the effect of aggregate size which plays very important role in the shear strength.

3.3.1.4. Bazant and Sun (1987):

Bazant and Sun (1987) further modified above model by incorporating the size of coarse aggregate as below

$$v_u = \left[0.54\sqrt[3]{\rho}\right]\times\left[\frac{1+\sqrt{\frac{5.08}{ag}}}{\sqrt{1+\frac{d}{25ag}}}\right]\times\left[\sqrt{f_c'}+249.2\sqrt{\frac{\rho}{(a/d)^5}}\right] MPa \qquad (3.4)$$

Where *ag* = Max. aggregate size.

3.3.1.5. British Standard BS 8110:1997

According to British code (BS code 8110:1997) the beam depth has been included for a/d > 2. The nominal shear strength of the beam is as follows

$$V_c = \left[\frac{0.79}{\gamma_m}\right]\times\left[\frac{100A_s}{bd}\right]^{\frac{1}{3}}\times\left[\frac{400}{d}\right]^{\frac{1}{4}}\times\left[\frac{f_{cu}}{25}\right]^{\frac{1}{3}} for\ \frac{a}{d}>2 \qquad (3.5)$$

$$V_c = \left(\frac{2d}{a}\right)\left[\frac{0.79}{\gamma_m}\right]\left[\frac{100A_s}{bd}\right]^{\frac{1}{3}}\times\left[\frac{400}{d}\right]^{\frac{1}{4}}\times\left[\frac{f_{cu}}{25}\right]^{\frac{1}{3}} for\ \frac{a}{d}<2 \qquad (3.5.a)$$

$$where \quad \frac{100A_s}{bd} \le 3, \frac{400}{d} \ge 1, \gamma_m = 1.25 \ \& \ f_{cu} \le 40MPa$$

However the drawback is that the depth of beam is limited to only 400 mm through the limit(400/d) ≥ 1 with compressive strength of concrete is less than or equal to 40 MPa and the percentage of the flexural reinforcement is 3.0 %.

3.3.2. Beam with web reinforcement

3.3.2.1. Indian Standard IS 456: 2000

As per IS 456:2000 total shear V_u resisted by beam is carried by two parts

- Shear resisted by concrete V_c
- Shear resisted by steel V_s

$$V_u = V_c + V_s \tag{3.6}$$

$$V_c = \delta \times \tau_c \times bd \quad \left(\text{where} \ \ \delta = 1 + \frac{3P_u}{A_g f_{ck}} \le 1.5 \right) \tag{3.7}$$

$$V_s = 0.87 f_y A_{sv} \frac{d}{s_v} \quad for\ vertical\ stirrups \tag{3.8}$$

$$V_s = 0.87 f_y A_{sv} \frac{d}{s_v} (\sin\alpha + \cos\alpha) \quad for\ inclined\ stirrups \tag{3.8.a}$$

3.3.2.2. American Standard ACI 318:2008

As per ACI 318:2008 total shear V_u resisted by beam is carried by two parts

- Shear resisted by concrete V_c
- Shear resisted by steel V_s

For normal weight concrete,

$$V_u = V_c + V_s \tag{3.9}$$

$$V_c = \delta \times \left(0.17\sqrt{f_c'}\right) \times bd \quad \left(\text{where, } \delta = 1 + \frac{P_u}{14A_g}\right) \tag{3.10}$$

$$V_s = \frac{A_{sv} \times f_{yh} \times d}{s_v} \quad \textit{for vertical stirrups} \tag{3.11}$$

$$V_s = \frac{A_{sv} \times f_{yh} \times d}{s_v}(\sin\alpha + \cos\alpha) \textit{ for inclined stirrups} \tag{3.11.a}$$

3.4. EXAMPLE OF SHEAR STRENGTH ESTIMATION

To compare the shear capacity equations available in literature a test beam section is considered and shear capacity for this beam section is calculated using all the equation presented above. The details of the test section are given below. Fig. 3.2 presents a sketch of the test beam considered for the comparison.

Details:

- Type of the beam: Simply supported beam subjected to one point load.
- Beam size = 150 × 250 mm with cover 25 mm.
- Span = 3 m.
- Shear span-to-depth ratio = 3.6
- Top reinforcement = 3 number of 12 mm bars (3Y12)
- Bottom reinforcement = 3 number of 16 mm bars (3Y16)
- Web reinforcement = 2 legged 8 mm stirrups at 150 mm c/c
- Shear span = 810 mm.
- Maximum aggregate size = 40 mm.
- Grade of Materials = M 20 grade of concrete and Fe 415 grade of reinforcing steel

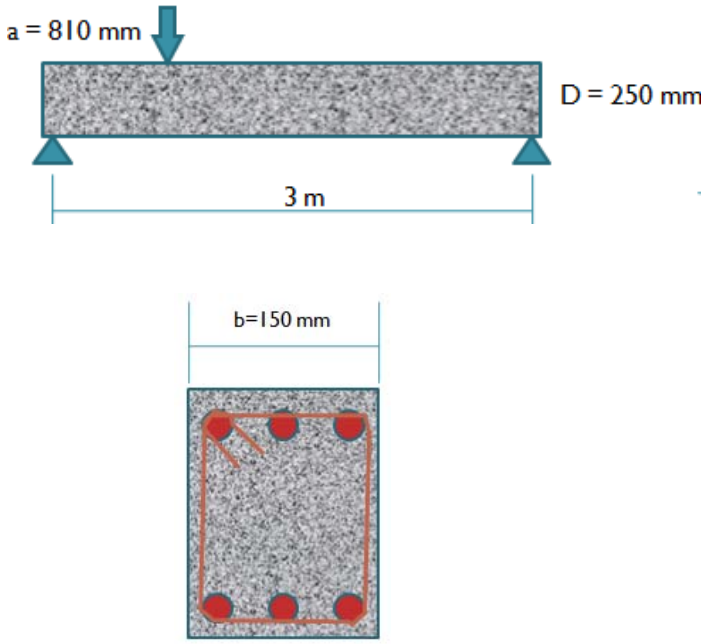

Fig. 3.2. Test beam section considered for the comparison.

Table 3.1 presents the shear capacity as carried out by the concrete and transverse reinforcement separately for different approaches available in literature.

Table 3.1. Ultimate shear strength (KN) of beam

Methods	**V_c (kN)**	**V_s (kN)**	**V_y (kN)**	**V_u (kN)**
Zsutty's T.C	32.87	-	-	-
Mphonde & Frantz	47.29	-	-	-
Bazant & Kim	34.56	-	-	-
Bazant & Sun	30.60	-	-	-
BS 8110 : 1997	27.71	--	-	-
IS 456:2000	30.10	54.42	-	84.52
ACI 318: 2008	22.95	62.55	-	85.50
FEMA - 356	0	$V_{s,y}$	$V_y=V_{s,y}$	$1.05V_y$

*For seismic loading.

3.5. SUMMARY

This chapter discusses briefly the existing models available for shear capacity estimation for sections with and without web reinforcement. Shear capacity calculations for structural member are included as well. From this chapter it can be calculated that FEMA-356 does not consider contribution of concrete in shear strength calculation for beam under earthquake loading. Contribution of web reinforcement in shear strength given in IS-456: 2000 and ACI-318: 2008 represent ultimate strength of the stirrups. FEMA-356 consider ultimate shear strength carried by the web reinforcement (= strength of the beam) as 1.05 times the yield strength hence no clarity in yield strength.

CHAPTER 4

SHEAR DISPLACEMENT MODEL

4.1. SHEAR DISPLACEMENT

Consider the reinforced concrete element shown in Fig.4.1. The shear forces are represented by *V*. The application of forces in such a manner causes the top of the element to slide with respect to the bottom. The displaced shape is shown by the dashed lines and the corresponding displacement is known as shear displacement depicted by (δ). Shear displacements over the height of the element are generally expressed in terms of shear strain (γ) which is ratio of shear displacement to height of the element and is a better representation of shear effect.

The effect of the shear forces translates into tension along the diagonal, which can be visualized by resolving the shear forces along the principal direction. As the concrete is weak in tension, it is susceptible to cracks in the direction perpendicular to the tensile load, which creates diagonal cracking well known to be associated with shear. The corresponding displacement is known as shear displacement (δ).

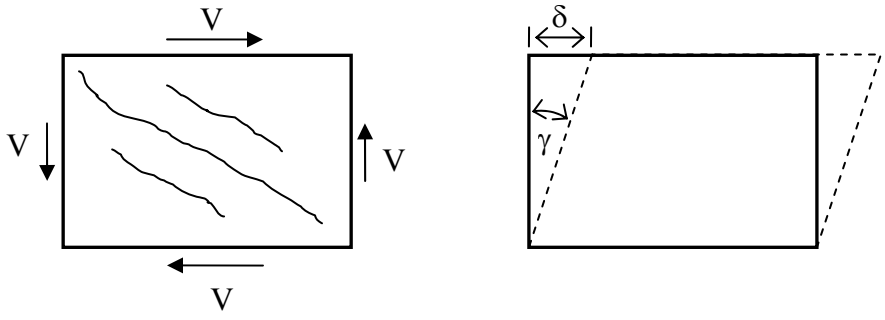

Fig 4.1. Shear displacement of concrete member

Deflections due to flexure and bond-slip are relatively easy to model with adequate accuracy whereas calculating shear displacement accurately has not been investigated thoroughly. The accuracy of the few existing models is not known. This chapter presents various methodologies available in literature to estimate shear displacement of RC section for un-cracked phase, at yield and at collapse.

4.1.1. Uncracked shear displacement

It is the shear displacement before and at the cracking point. This point is corresponding to the flexural cracking.

Uncracked shear stiffness K_{shear} is defined as slope of the shear force versus shear displacement relation.

$$\frac{V}{\Delta_{shear}} = \frac{GA}{L} \qquad (4.1)$$

Where V = shear force

Δ_{shear} = shear displacement before cracking.

Equation 4.1 assumes that shear stress distribution is uniform over the beam cross section, which is a reasonable assumption for reinforced concrete members. Thus the equation for uncracked shear displacement is given as

$$\Delta_{shear} = \frac{VL}{GA} \qquad (4.2)$$

This is, in fact, a well accepted and the commonly used theory to define relationship between shear force and shear displacement before cracking.

4.2. MODELS FOR SHEAR DISPLACEMENT AT YIELD

Most of the models available in literature are developed to predict shear displacement at yield point. The reason for concentrating on yield point is mainly because some of the shear strength models use displacement ductility as a measure of shear strength. Displacement ductility is defined as ratio of ultimate displacement to yield displacement. Thus it is necessary to predict displacement at yield more accurately with better knowledge of all its components including flexure, bar-slip and shear displacement. The following models are developed to calculate the shear displacement at yield. These models are applicable for both beam and column with web reinforcement.

4.2.1. Priestley et al. (1996)

It divides the shear displacement at yield into two components:

- shear carried by concrete Δ_{sc},
- transverse reinforcement mechanism Δ_{ss}.

This approach is similar to Park and Paulay (1975). The concrete component Δ_{sc} is defined as

$$\Delta_{sc} = \frac{2L\left(V_C + V_P\right)}{0.4E_C \times 0.8A_g} \tag{4.3}$$

Where L = beam length

A_g = gross cross-sectional area,

E_c = modulus of elasticity for concrete,

V_c and V_p = shear carried by concrete and axial load

$$V_C = 0.29 f_c^{1/2} 0.8A_g \tag{4.4}$$

$$V_P = P\tan\left(D - C\right)\alpha \tag{4.5}$$

Where P is the axial load, and K is a numerical factor, taken as 2 for single bending and 1 for double bending, c and D as defined in Fig. Shear displacement due to elongation of stirrups Δss , is defined by

$$\Delta_{ss} = \varepsilon_t L \tag{4.6}$$

Where ε_t = average elastic strain in the transverse reinforcement

$$\varepsilon_t = \frac{V_S S}{E_S A_V d} \tag{4.7}$$

Where A_v = area of transverse reinforcement.

$$V_S = V_{y'} - \left(V_C + V_p\right) \tag{4.8}$$

Where $V_{y'}$ = Shear force corresponding to yield.

If (Vc + Vp) should be smaller than the shear force corresponding to yield then Vy' to be used in Δ_{sc} equations .Else, $V_{y'}$ should be used instead of (Vc + Vp) .

4.2.2. Sezen (2002)

Sezen (2002) developed an equation based on measured shear displacements during the experimental investigation, by regression analysis using test data. The model takes into consideration the effect of axial load. The shear displacement at yield is defined as follows

$$\delta_{y\,shear} = \frac{3}{0.2 + 0.4P_r}\left(\frac{V_y L}{E_c A_g}\right) \tag{4.9}$$

Where $V_y = {2M_y}/{L}$ for double curvature

My = Yield moment capacity

Pr is axial load ratio defined as ratio of applied axial load (*P)* to the nominal axial load Capacity (*Po).*

4.2.3. Gerin and Adebar (2004)

The recent study by Gerin and Adebar (2004) expresses the yield shear displacement in terms of shear strain at yield, which is given by

$$\gamma_y = \frac{f_y}{E_s} + \frac{V_y - n}{\rho_v E_s} + \frac{4V_y}{E_c} \qquad (4.10)$$

Where f_y and E_s = yield stress and modulus of elasticity of reinforcement

V_y = applied shear stress at yield

ρ_v = transverse reinforcement ratio

n = axial stress with positive value for compression.

Also V_y by the ACI code (ACI 318-02) is

$$V_y = 0.25\sqrt{f_c'} + \rho_h f_y \qquad (4.11)$$

Where ρ_h is longitudinal reinforcement ratio. The model is applicable for columns with axial load ratio less than 0.15.

4.2.4. Lehman and Moehle (2000)

This model is not only limited to yield displacement; it also estimates force-shear deformation response until the loss of lateral load resisting capacity. This model adapts the uncracked shear displacement model .The beam height is divided into infinitesimal layers. The shear force throughout the length of beam is constant but the moment changes thus changing the concrete stress over beam height. The total shear displacement for the entire beam can be calculated as

$$\Delta_v = \int_L \frac{V(x)dx}{G_{eff}(x)A_{eff}(x)} = V\int_L \frac{dx}{G_{eff}(x)A_{eff}(x)} \qquad (4.12)$$

Where V is the constant shear force, $G_{eff}(x)$ and A_{eff} are effective shear modulus and effective cross sectional area at each plane.

$$G_{eff}(\mathrm{x}) = \frac{E_c(x)}{2(1+\mu)} \qquad (4.13)$$

Where $E_c(x)$ is elastic modulus of concrete at each plane, μ is Poisson's ratio taken as 0.3.

$$A_{eff} = \frac{R^2}{2}\left(\psi(x) - \sin(\psi(x))\right) \qquad (4.14)$$

$$\psi(x) = \cos\left(\frac{R - \left(\varepsilon_{cu}(x) \big/ (\varphi(x))\right)}{R}\right) \qquad (4.15)$$

With R is half of the radius, $\varphi(x)$ is the cross sectional curvature and $\varepsilon_{cu}(x)$ is corresponding maximum compressive strain. Thus, the shear displacement defined by this theory is a function of moment-curvature relationship.

4.2.5. Panagiotakos and Fardis (2001)

This model is based on statistical investigation of experimental results for a test database of over 1000 well-designed columns. To examine the shear displacements at yield, beam which did not exhibit bond slip displacements were selected from the database. The experimental average shear strains were then approximated as difference between the total measured average strain and calculated yield strain,

$$\theta_{y,flex} = \frac{\phi_y L_s}{3} \qquad (4.16)$$

Where L_s =shear span,

ϕ_y = Yield curvature = ε_c / c

Shear displacement at yield is given by:

$$\delta_{y\ shear} = 0.0025 L_s \qquad (4.17)$$

4.3. MODELS FOR ULTIMATE SHEAR DISPLACEMENT

The following models are developed to calculate the shear displacement at the maximum shear strength.

4.3.1. Park and Paulay (1975)

The theory of calculating ultimate shear displacement is based on truss analogy. This was actually proposed for concrete beams but has been commonly used for columns. A Concrete beam subjected to shear is modeled as shown in Fig. 4.2

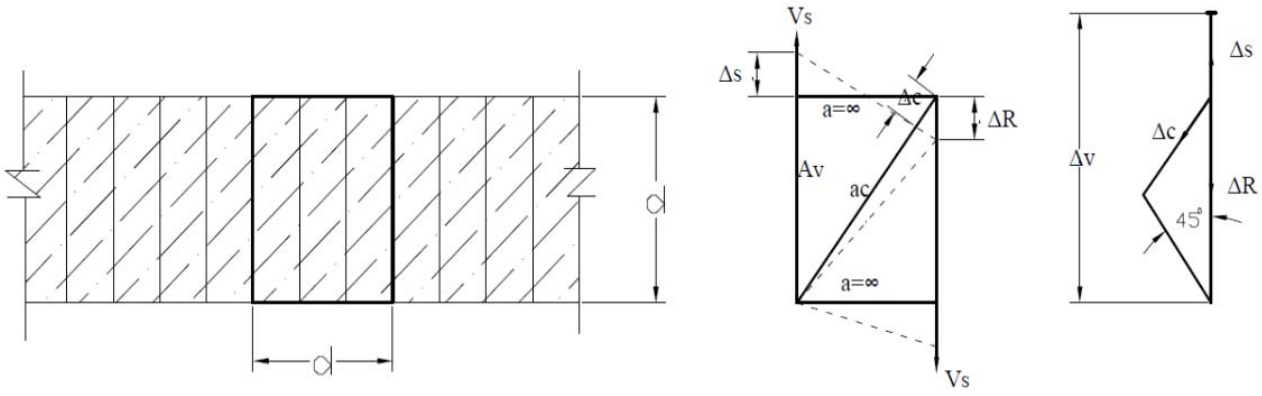

Fig 4.2. Shear displacement for beam (Park and Paulay 1975)

From geometry, shear displacement as,

$$\Delta_v = \Delta_s + \sqrt{2\Delta_c} \qquad (4.18)$$

Where $\Delta_c = \frac{2\sqrt{2}V_s}{E_c b_w}$ = Shortening of concrete (*i.e.* compression of struts)

$\Delta_s = \frac{V_s s}{E_s A_v}$ = Elongations of stirrups

Expressing the displacements in terms of the shear force resisted by stirrups V_s, Then shear distortion per unit length θ_v as

$$\theta_v = \frac{V_s}{E_s b_w d}\left(\frac{1}{\rho_v} + 4\eta\right) \qquad (4.19)$$

Where E_s = Modulus of elasticity for steel,

$n = {Es}/{Ec}$ = Modular ratio

b_w = Width of beam web

d = Effective depth

$\rho_v = \frac{A_v}{s b_w}$ = Transverse reinforcement ratio

It does not take into account the effect of axial load thus its use to predict the shear displacement of compression members should be avoided.

4.3.2. CEB (1985)

Comite Euro-International du Beton (CEB) (1985) uses the theory proposed by Park and Paulay (1975) with a change for the value of shear force. It can be noted that shear distortion per unit length uses amount of shear resisted by stirrups V_s, whereas CEB suggests to use the total shear force V that includes contribution of stirrups as well as concrete.

4.3.3. Gerin and Adebar (2004)

Ultimate shear displacement can be obtained in terms of ultimate shear strain γ_y in this mode. As given by Equation proposed for shear strain ductility μ_y based on investigation of expt. data

$$\mu_y = \frac{\gamma_u}{\gamma_y} = 4 - 12\frac{v_y}{f_c'} \qquad (4.20)$$
$$here \;\; v_y \le 0.25 fc'$$

Where γ_y is the yield shear strain and υ_y is the yield shear stress.

4.4. CALCULATIONS FOR YIELD AND ULTIMATE SHEAR DISPLACEMENT

To compare equations available in literature for estimation of shear displacement at yield and ultimate point, a test beam section is considered and shear displacement for this beam section is calculated using all the equation presented above. The details of the test section are given below. A sketch of the beam section is presented in Fig. 4.3.

Details:

- Type of the Section: Simply supported beam subjected to one point load.
- Beam size = 150 × 250 mm with cover 25 mm.
- Span = 3 m.
- Shear span to depth ratio = 3.6
- Top reinforcement = 3 numbers of 12 mm bars (3Y12)
- Bottom reinforcement = 3 numbers of 16 mm bars (3Y16)
- Web reinforcement = 2 legged 8 mm stirrups at 150 mm c/c
- Shear span = 810 mm.
- Maximum aggregate size = 40 mm.

- Grade of materials = M 20 grade of concrete and Fe 415 grade of reinforcing steel.

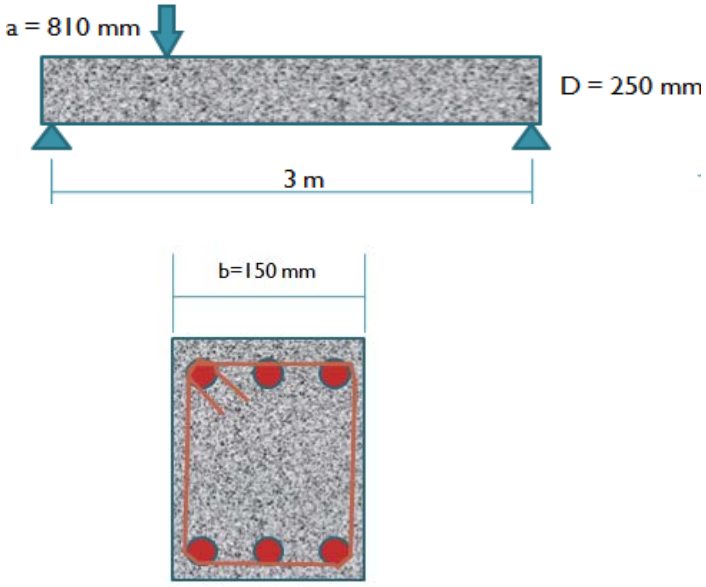

Fig. 4.3. Test beam section considered for the comparison.

Table 4.1 presents the shear displacement at yield and ultimate point for different approaches available in literature.

Table 4.1. Ultimate shear displacement (mm) of beam

Methods	Δ_y (mm)	Δ_u (mm)
Priestley et.al (1996)	2.953	-
Sezen (2002)	1.505	-
Gerin and adebar (2004)	12.006×10^{-3}	NA
Panagiotakos and Fardis (2001)	2.025	-
Park and Paulay (1975)	-	4.128
CEB (1985)	-	5.856

4.5. SUMMARY

Estimation of shear displacement capacity of RC section is an important part of the nonlinear shear failure modelling. There are very few published literatures available on this area. Chapter 4 presents the existing models available for shear displacement at yield and ultimate. Shear displacement calculation for structural member using available methods are also demonstrated through a case study. The model by Sezen (2002) is based on regression analysis of test data. Model by Panagiotakos and Fardis (2001) is simple but it is reported to be overestimating the shear displacement. Model proposed by Gerin and Adebar (2004) is reported to be underestimating the shear displacements at yeild. Models proposed by Park and Paulay (1975) and CEB (1985) are reported to be effective in predicting the ultimate shear displacements. Model by Gerin and Adebar (2004) is reported to be not suitable for predicting the ultimate shear displacements.

CHAPTER 5

STRUCTURAL MODELLING

5.1. INTRODUCTION

In the present study an existing building is selected for seismic evaluation case study. This building is analyzed considering nonlinear flexural and shear failure of the frame elements. Shear failure model is developed from the existing literature presented in the previous chapters. The building is also analyzed ignoring the shear failure of the frame elements for demonstrating the importance of shear failure model in seismic evaluation study. All the analyses are carried out in commercial software SAP 2000.

Developing computational model is an important part on which linear or nonlinear, static or dynamic analysis performed. First part of this chapter explains the details of computational model. Also, details of the selected building model are described in this section. Accurate modeling of the nonlinear properties of various structural elements is very important in nonlinear analysis. Frame elements in this study are modelled with inelastic flexural hinges and shear hinges. The procedure to generate these hinge properties and its related assumptions are briefly explained in the second part of this chapter.

5.2. COMPUTATIONAL MODEL

Modeling a building consist of the modeling and assemblage of its various load-carrying

elements. A model must represent the 3D characteristics of building, including mass distribution, strength, stiffness and deformability. Modeling of the material properties and structural elements used in the present study is discussed below.

5.2.1 Material Properties

The material properties of any member consists of its mass, unit weight ,modulus of elasticity, poisson's ratio, shear modulus and coefficient of thermal expansions.The material grades used for frame model are presented in Table 5.1.

Table 5.1 Materials Grades

Material	Grade
Concrete	M 20
Reinforcing steel	Fe 415

Elastic material properties of these materials are taken as per Indian Standard IS 456: 2000. The short-term modulus of elasticity (E_c) of concrete is taken as:

$$\mathrm{E_c} = 5000\sqrt{f_{ck}}MPa \qquad (5.1)$$

f_{ck} is the characteristic compressive strength of concrete cube in MPa at 28-day (25 MPa in this case). For the steel rebar, yield stress (f_y) and modulus of elasticity (E_s) is taken as per IS 456 (2000).

5.2.2. Structural Elements

Beams and columns are modelled by 3D frame elements. To obtain the bending moments and forces at the beam and column faces beam-column joints are modelled by giving end-

offsets to the frame elements. The beam-column joints are as considered to be rigid (Fig.5.1). The column end at foundation assumed as fixed for all the models in this study. Nonlinear properties at the possible yield locations are to be considered for all the frame elements.

By assigning 'diaphragm' action at each floor level the structural effect of slabs due to their in-plane stiffness is taken into account. The mass/weight contribution of slab is modelled separately on the supporting beams.

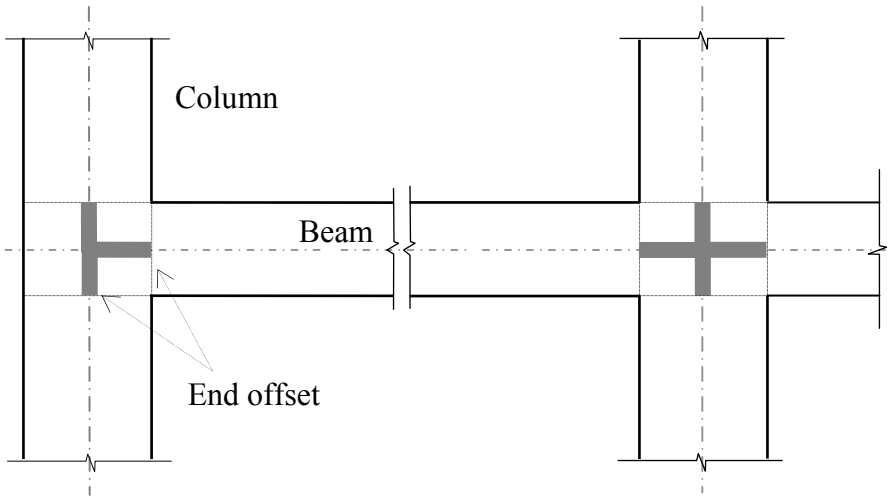

Fig.5.1. Use of end offsets at beam-column joint

5.3. BUILDING GEOMETRY

The selected building is a three storey residential apartment building located in Seismic Zone III designed with IS 1893:2002 and IS 456:2000. Table 5.2 presents a summary of the building parameters. The building is almost symmetric in both the directions. The concrete slab is 150 mm thick at every floor level. The wall thickness is 230mm for the exterior and 120mm for interior walls.

Table 5.2. Building summary

Building Type	RC frame with un-reinforced brick infill
Year of construction	2001
Number of stories	Ground + 3 Storey
Plan dimensions	20.50m × 13.30m
Building height	13.1 m above plinth level

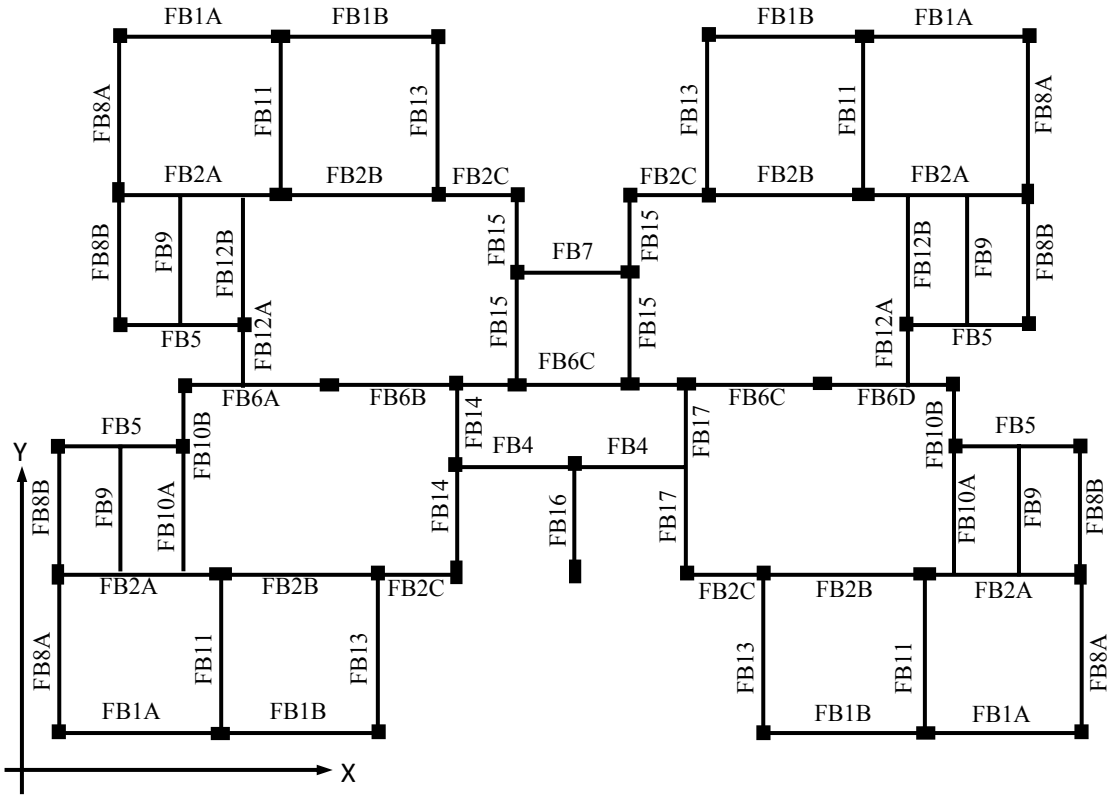

Fig.5.2. Floor (for Plinth, Ground, First and Second) framing plan – Beam location

The floor plan is same up to fourth floor. At the plinth level few beams are absent. The beam layout for plinth, first three floors and the roof are shown in Figure 5.2 and Figure

5.3 respectively. Figure 5.4 shows the column locations. The front view, side view elevation and 3D Model of the building are shown in Figure 5.5, Figure 5.6 and Figure 5.7 respectively. Table 5.3 and Table 5.4 provide the size and reinforcement details for beam and column sections. The foundation system is isolated footing. The footings are located 1.23m below the plinth level. Details of the foundation are given in Table 5.5. Typical plan and elevation of the footing is shown in Fig. 5.8.

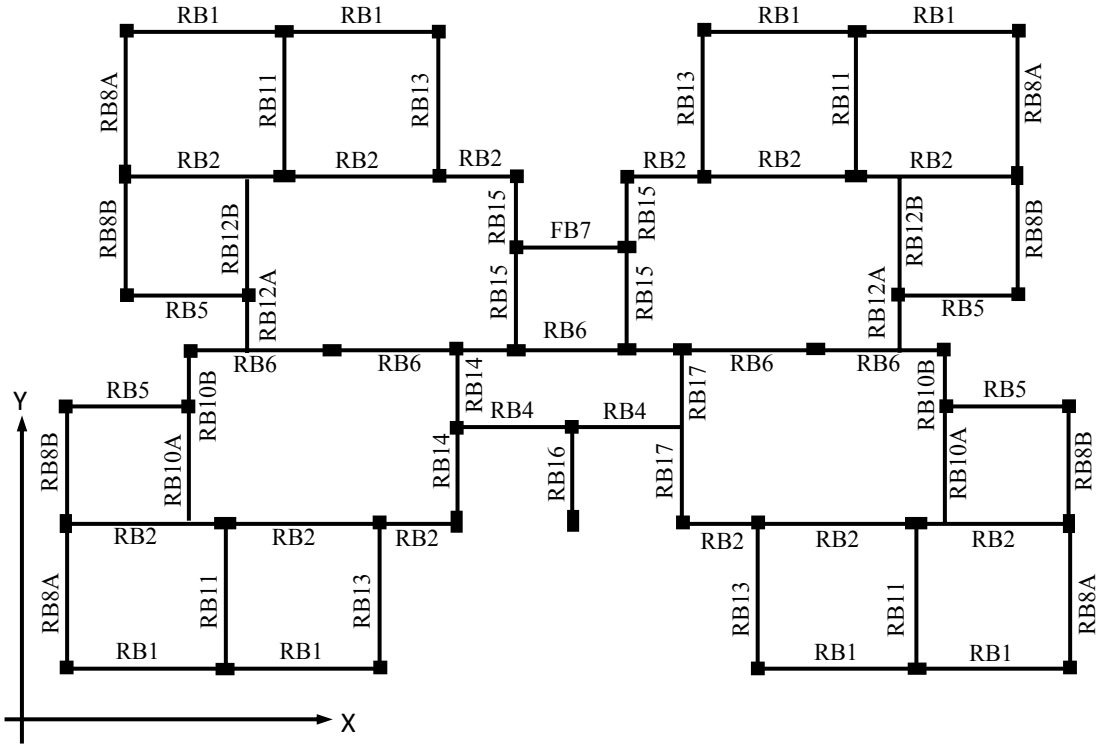

Fig.5.3. Roof framing plan – Beam location

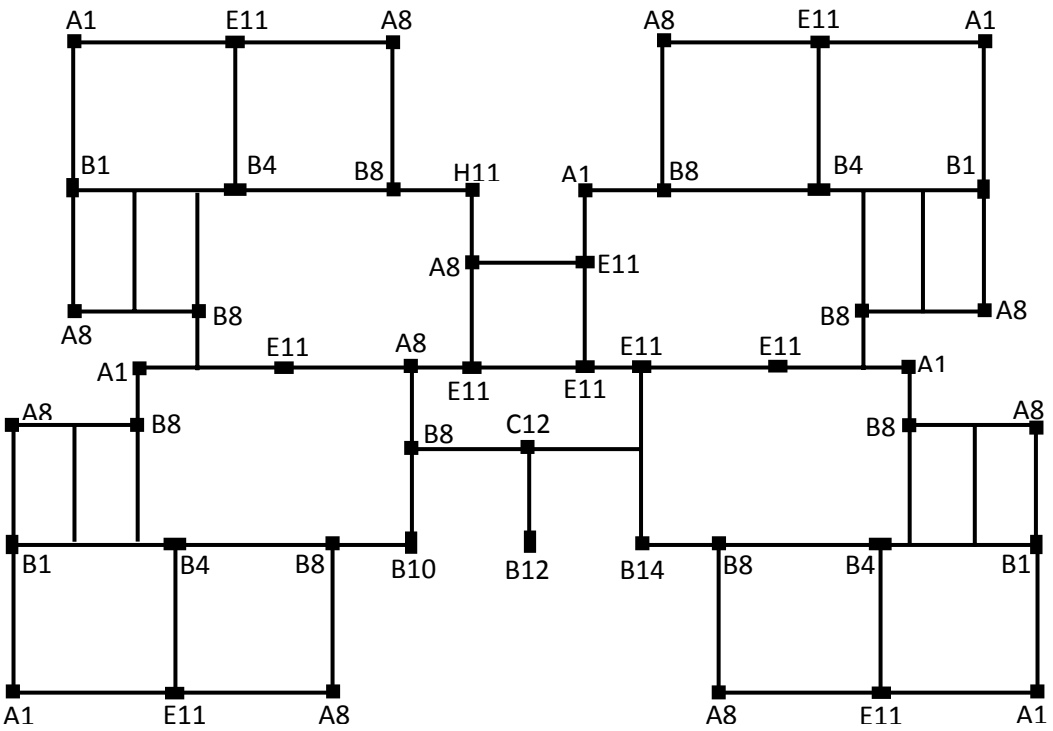

Fig.5.4. Column location

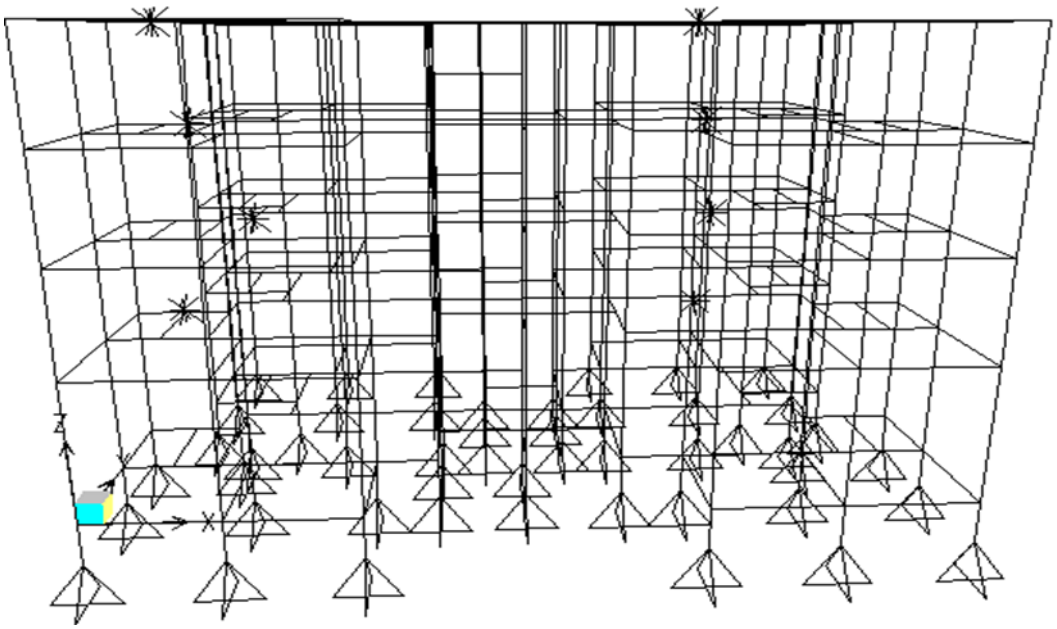

Fig.5.5. Elevation of the building – Front view

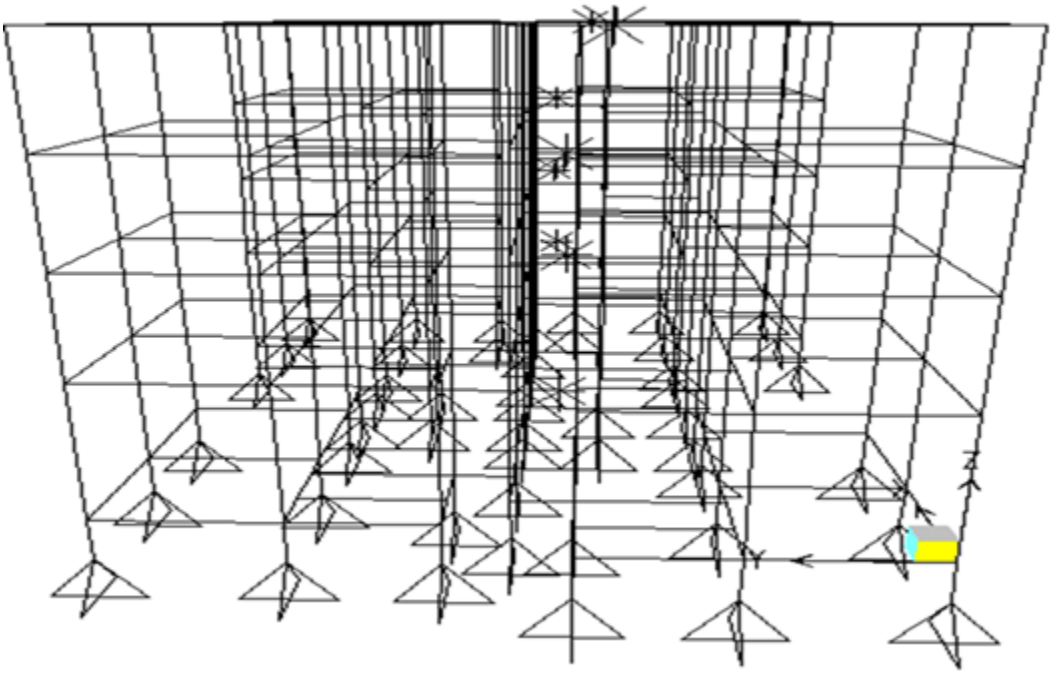

Fig.5.6. Elevation of the building – Side view

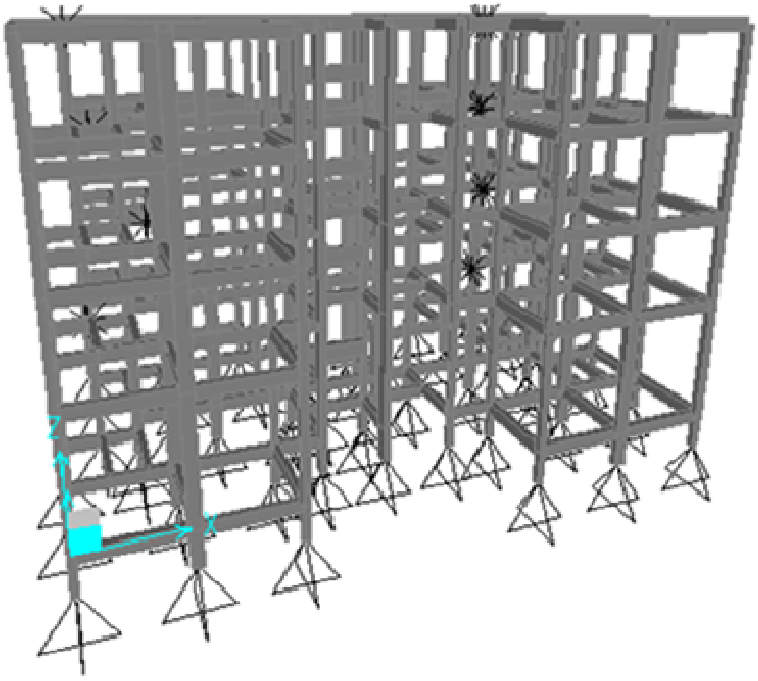

Fig.5.7. 3D computer model of the building

Table 5.3. Details of beam sections

Plinth ,Ground, First and Second floor level				
FB1A	230 × 400	2Y12	2Y12	2Y8 @ 200 c/c
FB1B	230 × 400	3Y12	2Y12	2Y8 @ 200 c/c
FB2A	230 × 400	3Y12	3Y12	2Y8 @ 200 c/c
FB2B	230 × 400	3Y12	2Y12	2Y8 @ 200 c/c
FB2C	230 × 400	3Y12	3Y12	2Y8 @ 200 c/c
FB4	230 × 400	2Y12	2Y12	2Y8 @ 200 c/c
FB5	230 × 400	3Y12	3Y12	2Y8 @ 200 c/c
FB6A	230 × 400	2Y12	2Y12	2Y8 @ 200 c/c
FB6B	230 × 400	3Y12	2Y12	2Y8 @ 200 c/c
FB6C	230 × 400	2Y12	2Y12	2Y8 @ 200 c/c
FB6D	230 × 400	3Y12	3Y12	2Y8 @ 200 c/c
FB10A	230 × 400	2Y12	2Y12	2Y8 @ 200 c/c
FB10B	230 × 400	3Y12	2Y12	2Y8 @ 200 c/c
FB11	230 × 400	3Y12	2Y12	2Y8 @ 200 c/c
FB12A	230 × 400	3Y12	3Y12	2Y8 @ 200 c/c
FB12B	230 × 400	3Y12	3Y12	2Y8 @ 200 c/c
FB13	230 × 400	2Y12	2Y12	2Y8 @ 200 c/c
FB14	230 × 400	2Y12	2Y12	2Y8 @ 200 c/c
FB15	230 × 400	2Y12	2Y12	2Y8 @ 200 c/c
FB16	230 × 400	3Y12	2Y12	2Y8 @ 200 c/c
FB17	230 × 400	3Y12	2Y12	2Y8 @ 200 c/c
FB7	230 × 400	2Y12	2Y12	2Y8 @ 200 c/c
FB8A	230 × 400	2Y12	2Y12	2Y8 @ 200 c/c
FB8B	230 × 400	2Y12	2Y12	2Y8 @ 200 c/c
FB9	230 × 400	2Y12	2Y12	2Y8 @ 200 c/c
MB2	230 × 550	2Y12	2Y12	2Y8 @ 150 c/c

Table 5.3.(contd) Details of beam sections

Roof level				
RB1A	230 × 400	2Y12	2Y12	2Y8 @ 200 c/c
RB1B	230 × 400	2Y12	2Y12	2Y8 @ 200 c/c
RB2A	230 × 400	2Y12	2Y12	2Y8 @ 200 c/c
RB2B	230 × 400	2Y12	2Y12	2Y8 @ 200 c/c
RB2C	230 × 400	2Y12	2Y12	2Y8 @ 200 c/c
RB4	230 × 400	2Y12	2Y12	2Y8 @ 200 c/c
RB5	230 × 400	2Y12	2Y12	2Y8 @ 200 c/c
RB6A	230 × 400	2Y12	2Y12	2Y8 @ 200 c/c
RB6B	230 × 400	3Y12	2Y12	2Y8 @ 200 c/c
RB6C	230 × 400	2Y12	2Y12	2Y8 @ 200 c/c
RB6D	230 × 400	3Y12	2Y12	2Y8 @ 200 c/c
RB8A	230 × 400	3Y12	2Y12	2Y8 @ 200 c/c
RB8B	230 × 400	3Y12	2Y12	2Y8 @ 200 c/c
RB10A	230 × 400	3Y12	2Y12	2Y8 @ 200 c/c
RB10B	230 × 400	3Y12	2Y12	2Y8 @ 200 c/c
RB11	230 × 400	2Y12	2Y12	2Y8 @ 200 c/c
RB12A	230 × 400	2Y12	2Y12	2Y8 @ 200 c/c
RB12B	230 × 400	2Y12	2Y12	2Y8 @ 200 c/c
RB13	230 × 400	2Y12	2Y12	2Y8 @ 200 c/c
RB14	230 × 400	2Y12	2Y12	2Y8 @ 200 c/c
RB15	230 × 400	2Y12	2Y12	2Y8 @ 200 c/c
RB16	230 × 400	3Y12	2Y12	2Y8 @ 200 c/c
RB17	230 × 400	3Y12	2Y12	2Y8 @ 200 c/c
RB7	230 × 400	2Y12	2Y12	2Y8 @ 200 c/c

Table 5.4. Details of column sections

Column Number	Size (mm)	Longitudinal Reinforcement	Transverse Reinforcement
A8	230 × 230	4Y12	Y8 @ 190c/c
H11	230 × 230	4Y16	Y8 @ 190c/c
H111	230 × 230	4Y12	Y8 @ 190c/c
C12	230 × 230	4Y16, 2Y12	Y8 @ 190c/c
C121	230 × 230	4Y16	Y8 @ 190c/c
B14	230 × 230	4Y20, 2Y12	Y8 @ 190c/c
B141	230 × 230	4Y16, 2Y12	Y8 @ 190c/c
B8	230 × 230	6Y12	Y8 @ 190c/c
B81	230 × 230	4Y12	Y8 @ 190c/c
A1	230 × 230	6Y16	Y8 @ 190c/c
A11	230 × 230	4Y16, 2Y12	Y8 @ 190c/c
E11	230 × 380	4Y16, 2Y12	Y8 @ 190c/c
B4	230 × 450	4Y16, 2Y12	Y8 @ 190c/c
B12	230 × 450	6Y16	Y8 @ 190c/c
B121	230 × 450	6Y16, 2Y12	Y8 @ 190c/c
B10	230 × 450	6Y16, 2Y12	Y8 @ 190c/c
B101	230 × 450	6Y16	Y8 @ 190c/c
B1	380 × 230	4Y16, 2Y12	Y8 @ 190c/c

Table 5.5. Details of footings

Sl No	Name of footing	Size (mm)		Size (mm)		Reinforcement	Pedestal Size
		Length (L)	Breadth (B)	Edge Depth	H1		
1	F-1	1050	1050	150	250	10 Y@ 200 c/c B/W	380 × 380
2	F-2	1150	1150	150	300	10Y @ 200 c/c B/W	380 × 380
3	F-3	1250	1250	150	350	10 Y@ 200 c/c B/W	380 × 380
4	F-4	1350	1350	150	350	10 Y@ 180 c/c B/W	380 × 380
5	F-5	1600	1600	200	450	10 Y@ 170 c/c B/W	380 × 480
6	F-6	1700	1700	200	450	10 Y@ 150 c/c B/W	380 × 550
7	F-7	1800	1800	200	500	10 Y@ 160 c/c B/W	380 × 550

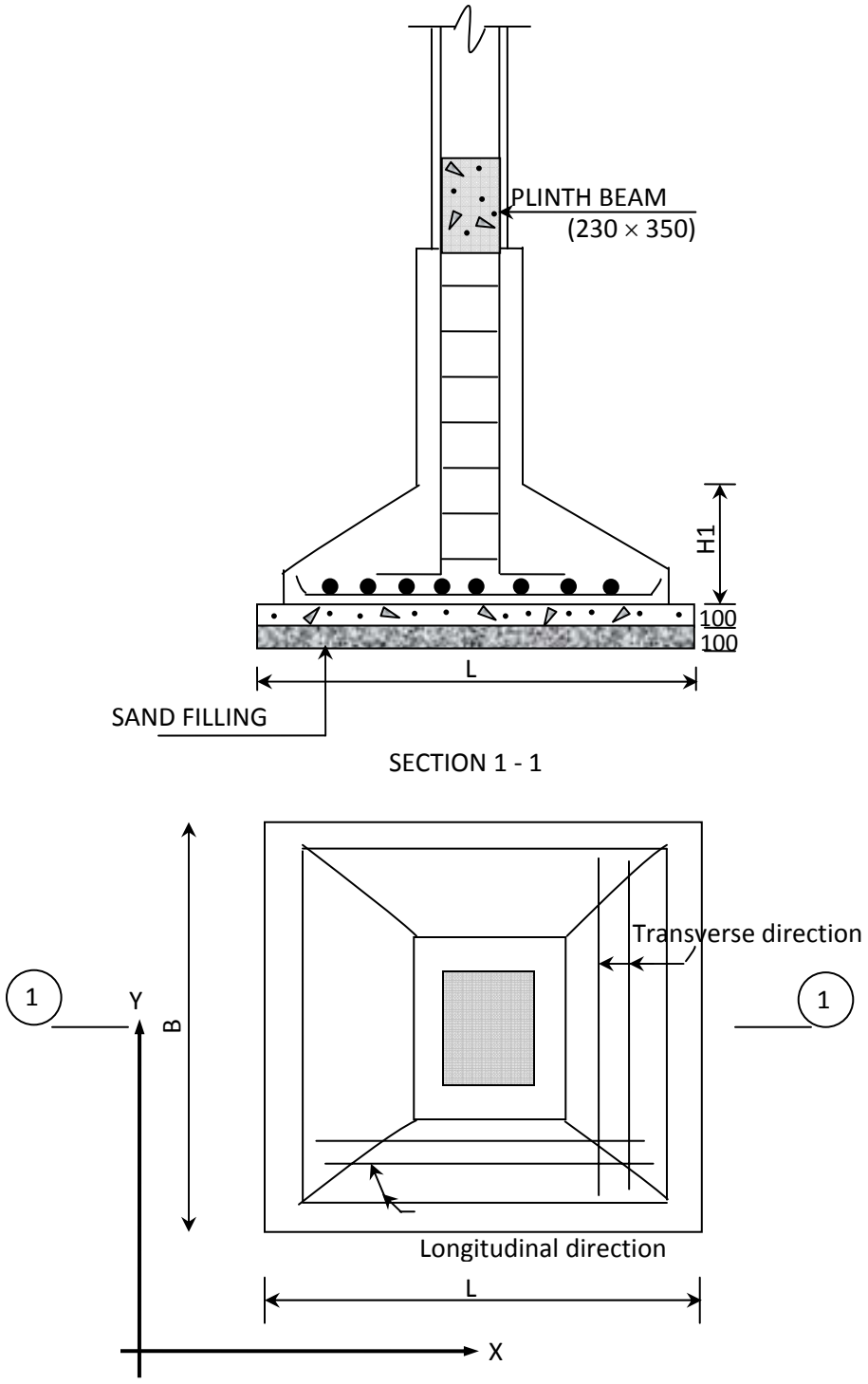

Fig.5.8. Typical plan of footing

5.4. MODELLING OF FLEXURAL HINGES

In the implementation of pushover analysis, the model must account for the nonlinear behaviour of the structural elements. In the present study, a point-plasticity approach is considered for modelling nonlinearity, wherein the plastic hinge is assumed to be concentrated at a specific point in the frame member under consideration. Beam and column elements in this study were modelled with flexure (M3for beams and P-M2-M3 for columns) hinges at possible plastic regions under lateral load (i.e., both ends of the beams and columns).Properties of flexure hinges must simulate the actual response of reinforced concrete components subjected to lateral load. In the present study the plastic hinge properties are calculated by SAP 2000. The analytical procedure used to model the flexural plastic hinges are explained below.

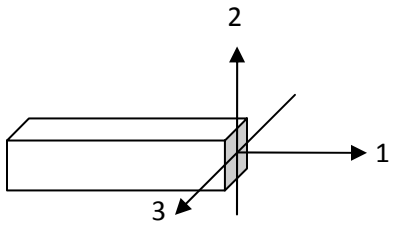

Fig.5.9. The coordinate system used to define the flexural and shear hinges

Flexural hinges in this study are defined by moment-rotation curves calculated based on the cross-section and reinforcement details at the possible hinge locations. For calculating hinge properties it is required to carry out moment–curvature analysis of each element. Constitutive relations for concrete and reinforcing steel, plastic hinge length in structural element are required for this purpose. The flexural hinges in beams are modelled with uncoupled moment (M3) hinges whereas for column elements the flexural hinges are modelled with coupled P-M2-M3 properties that include the interaction of axial force and bi-axial bending moments at the hinge location. Although the axial force interaction is

considered for column flexural hinges the rotation values were considered only for axial force associated with gravity load.

5.4.1. Stress-Strain Characteristics for Concrete

The stress-strain curve of concrete in compression forms the basis for analysis of any reinforced concrete section. The characteristic and design stress-strain curves specified in most of design codes (IS 456: 2000, BS 8110) do not truly reflect the actual stress-strain behaviour in the post-peak region, as (for convenience in calculations) it assumes a constant stress in this region (strains between 0.002 and 0.0035). In reality, as evidenced by experimental testing, the post-peak behaviour is characterised by a descending branch, which is attributed to 'softening' and micro-cracking in the concrete. Also, models as per these codes do not account for strength enhancement and ductility due to confinement. However, the stress-strain relation specified in ACI 318M-02 consider some of the important features from actual behaviour. A previous study (Chugh, 2004) on stress-strain relation of reinforced concrete section concludes that the model proposed by Panagiotakos and Fardis (2001) represents the actual behaviour best for normal-strength concrete. Accordingly, this model has been selected in the present study for calculating the hinge properties. This model is a modified version of Mander's model (Mander*et. al.*, 1988) where a single equation can generate the stress f_c corresponding to any given strainε_c:

$$f_c = \frac{f'_{cc} x r}{r - 1 + x^r} \tag{5.2}$$

where, $x = \frac{\epsilon_c}{\epsilon_{cc}}; r = \frac{E_c}{E_c - E_{sec}}; E_c = 5000\sqrt{f'_{co}}; E_{sec} = \frac{f'_{cc}}{\varepsilon_{cc}}$ and f'_{cc} is the peak strength expressed as follows:

$$f'_{cc} = f'_{co}\left[1 + 3.7\left(\frac{0.5k_e\rho_s f_y h}{f'_{co}}\right)^{0.85}\right] \tag{5.3}$$

The expressions for critical compressive strains are expressed in this model as follows:

$$\varepsilon_{cu} = 0.004 + \frac{0.6\rho_s f_{yh}\epsilon_{sm}}{f'_{cc}} \tag{5.4}$$

$$\varepsilon_{cc} = \epsilon_{co}\left[1 + 5\left(\frac{f'_{cc}}{f'_{co}} - 1\right)\right] \tag{5.5}$$

The unconfined compressive strength (f'_{co}) is 0.75 f_{ck}, k_e having a typical value of 0.95 for circular sections and 0.75 for rectangular sections.

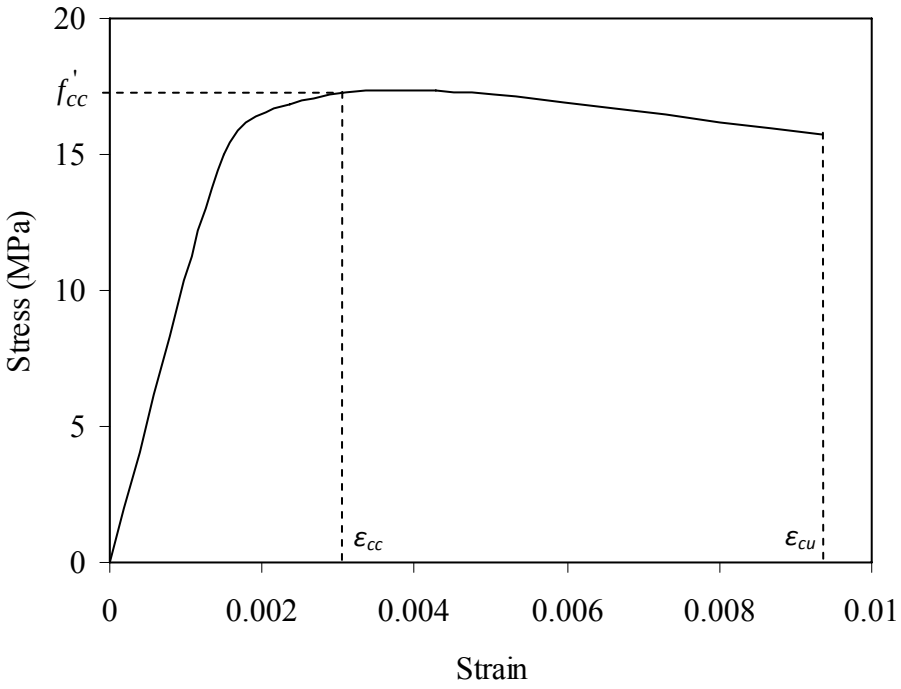

Fig.5.10. Typical stress-strain curve for M-20 grade concrete (Panagiotakos and Fardis, 2001)

Fig. 5.10 shows a typical plot of stress-strain characteristics for M-20 grade of concrete as per Modified Mander's model (Panagiotakos and Fardis, 2001). The advantage of using this model can be summarized as follows:

- A single equation defines the stress-strain curve (both the ascending and descending branches) in this model.
- The same equation can be used for confined as well as unconfined concrete sections.
- The model can be applied to any shape of concrete member section confined by any kind of transverse reinforcement (spirals, cross ties, circular or rectangular hoops).
- The validation of this model is established in many literatures (*e.g.*, Pam and Ho, 2001).

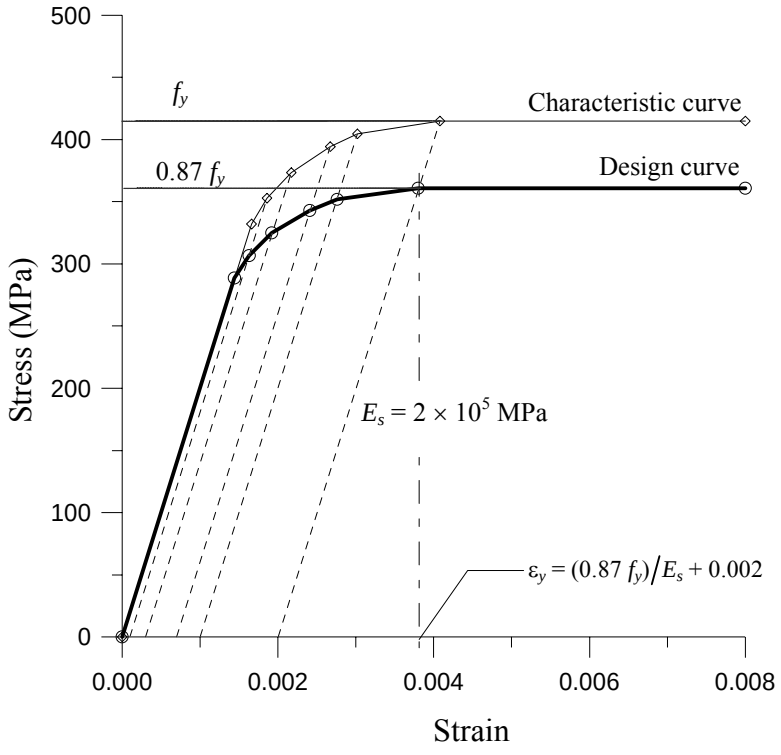

Fig.5.11. Stress-strain relationship for reinforcement – IS 456 (2000)

5.4.2. Stress-Strain Characteristics for Reinforcing Steel

The constitutive relation for reinforcing steel given in IS 456 (2000) is well accepted in literature and hence considered for the present study. The 'characteristic' and 'design' stress-strain curves specified by the Code for Fe-415 grade of reinforcing steel (in tension or compression) are shown in Fig. 5.11.

5.4.2. Moment-Curvature Relationship

Moment-curvature relation is a basic tool in the calculation of deformations in flexural members. It has an important role to play in predicting the behaviour of reinforced concrete (RC) members under flexure. In nonlinear analysis, it is used to consider secondary effects and to model plastic hinge behaviour.

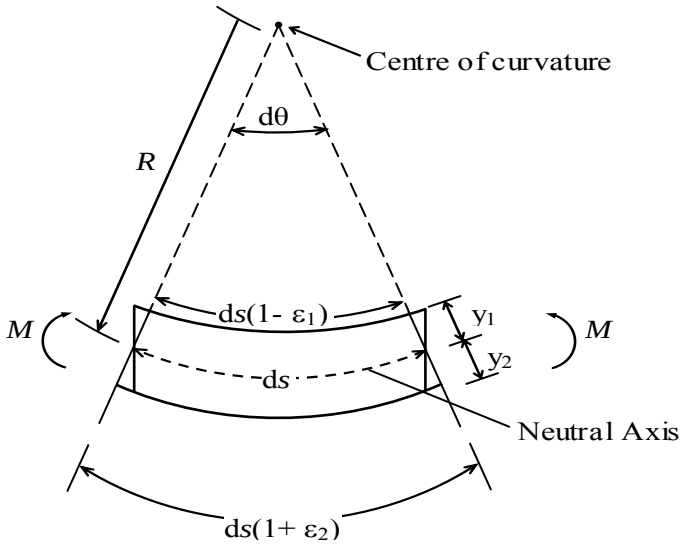

Fig.5.12. Curvature in an initially straight beam section (Pillai and Menon, 2006)

Curvature (φ) is defined as the reciprocal of the radius of curvature (R) at any point along a curved line. When an initial straight beam segment is subject to a uniform bending

moment throughout its length, it is expected to bend into a segment of a circle with a curvature φ that increases in some manner with increase in the applied moment (M). Curvature φ may be alternatively defined as the angle change in the slope of the elastic curve per unit length $\left(\varphi = 1/R = d\theta/ds\right)$. At any section, using the 'plane sections remain plane' hypothesis under pure bending, the curvature can be computed as the ratio of the normal strain at any point across the depth to the distance measured from the neutral axis at that section (Fig. 5.12).

If the bending produces extreme fibre strains of ε_1 and ε_2 at top and bottom at any section as shown in Fig. 5.12 (compression on top and tension at bottom assumed in this case), then, for small deformations, it can be shown that $\varphi = \left(\varepsilon_1 + \varepsilon_2\right)/D$. If the beam behaviour is linear elastic, then the moment-curvature relationship is linear, and the curvature is obtained as

$$\varphi = \frac{M}{EI} \tag{5.6}$$

The flexural rigidity (EI) of the beam is obtained as a product of the modulus of elasticity *E* and the second moment of area of the section *I*.

When an RC flexural member is subjected to a gradually increasing moment, it's behaviour transits through various stages, starting from the initial un-cracked state to the ultimate limit state of collapse. The stresses in the tension steel and concrete go on increasing as the moment increases. The behaviour at the ultimate limit state depends on the percentage of steel provided, i.e., on whether the section is 'under-reinforced' or 'over-reinforced'. In the case of under-reinforced sections, failure is triggered by yielding of tension steel whereas in over-reinforced section the steel does not yield at the

limit state of failure. In both cases, the failure eventually occurs due to crushing of concrete at the extreme compression fibre, when the ultimate strain in concrete reaches its limit. Under-reinforced beams are characterised by 'ductile' failure, accompanied by large deflections and significant flexural cracking. On the other hand, over-reinforced beams have practically no ductility, and the failure occurs suddenly, without the warning signs of wide cracking and large deflections.

In the case of a short column subject to uni-axial bending combined with axial compression, it is assumed that Eq. 5.6 remains valid and that "plane sections before bending remain plane". However, the ultimate curvature (and hence, ductility) of the section is reduced as the compression strain in the concrete contributes to resisting axial compression in addition to flexural compression.

5.4.3. Modelling of Moment-Curvature in RC Sections

Using the Modified Mander model of stress-strain curves for concrete (Panagiotakos and Fardis, 2001) and Indian Standard IS 456 (2000) stress-strain curve for reinforcing steel, for a specific confining steel, moment curvature relations can be generated for beams and columns (for different axial load levels). The assumptions and procedure used in generating the moment-curvature curves are outlined below.

Assumptions

i. The strain is linear across the depth of the section ('plane sections remain plane').

ii. The tensile strength of the concrete is ignored.

iii. The concrete spalls off at a strain of 0.0035.

iv. The initial tangent modulus of the concrete, E_c is adopted from IS 456 (2000), as $5000\sqrt{f_{ck}}$.

v. In determining the location of the neutral axis, convergence is assumed to be reached within an acceptable tolerance of 1%.

Algorithm for Generating Moment-Curvature Relation

i. Assign a value to the extreme concrete compressive fibre strain (normally starting with a very small value).

ii. Assume a value of neutral axis depth measured from the extreme concrete compressive fibre.

iii. Calculate the strain and the corresponding stress at the centroid of each longitudinal reinforcement bar.

iv. Determine the stress distribution in the concrete compressive region based on the Modified Mander stress-strain model for given volumetric ratio of confining steel. The resultant concrete compressive force is then obtained by numerical integration of the stress over the entire compressive region.

v. Calculate the axial force from the equilibrium and compare with the applied axial load (for beam element both of these will be zero). If the difference lies within the specified tolerance, the assumed neutral axis depth is adopted. The moment capacity and the corresponding curvature of the section are then calculated. Otherwise, a new neutral axis is determined from the iteration (using bisection method) and steps (iii) to (v) are repeated until it converges.

vi. Assign the next value, which is larger than the previous one, to the extreme concrete compressive strain and repeat steps (ii) to (v).

vii. Repeat the whole procedure until the complete moment-curvature is obtained.

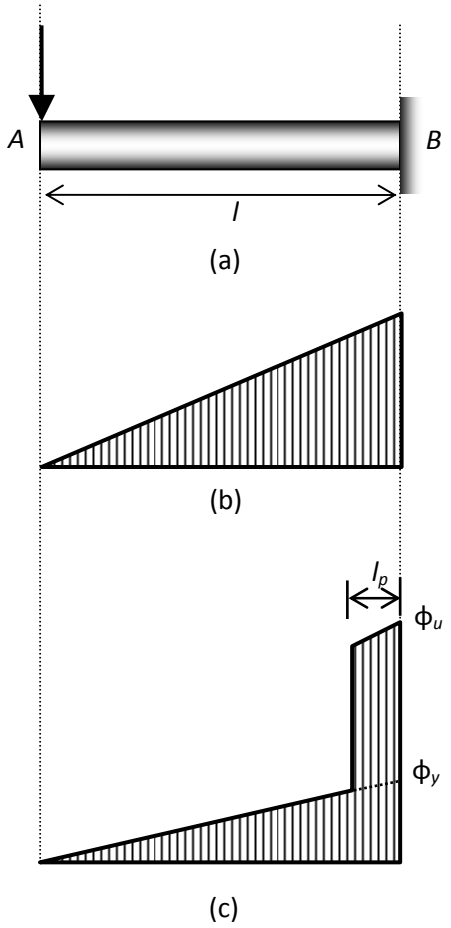

Fig.5.13. (a) cantilever beam, (b) Bending moment distribution, and (c) Curvature distribution (Park and Paulay 1975)

5.4.4. Moment-Rotation Parameters

Moment-rotation parameters are the actual input for modelling the hinge properties and this can be calculated from the moment-curvature relation. This can be explained with a simple cantilever beam AB shown in Fig. 5.13 (a) with a concentrated load applied at the

free end B. To determine the rotation between the ends an idealized inelastic curvature distribution and a fully cracked section in the elastic region may be assumed. Figs. 5.13 (b) and 5.13(c) represent the bending moment diagram and probable distribution of curvature at the ultimate moment.

The rotation between *A* and *B* is given by

$$\theta = \int_{A}^{B} \varphi \, dx \tag{5.7}$$

The ultimate rotation is given by,

$$\theta_u = \varphi_y \frac{1}{2} + (\varphi_u - \varphi_y) l_p \tag{5.8}$$

The yield rotation is,

$$\theta_y = \varphi_y \frac{1}{2} \tag{5.9}$$

And the plastic rotation is,

$$\theta_p = (\varphi_u - \varphi_y) l_p \tag{5.10}$$

l_p is equivalent length of plastic hinge over which plastic curvature is considered to be constant. The physical definition of the plastic hinge length, considering the ultimate flexural strength developing at the support, is the distance from the support over which the applied moment exceeds the yield moment. A good estimate of the effective plastic hinge length may be obtained from the following equation (Paulay and Priestley, 1992)

$$l_p = 0.08l + 0.15 d_b f_y \tag{5.11}$$

The yield strength of the longitudinal reinforcement should be in 'ksi'. For typical beam and column proportions Eq. 5.11 results in following equation (FEMA-274; Paulay and Priestley, 1992) where *D* is the overall depth of the section.

$$l_p = 0.5D \tag{5.12}$$

The moment-rotation curve can be idealised as shown in Fig. 5.14 and can be derived from the moment-curvature relation. The main points in the moment-rotation curve shown in the figure can be defined as follows:

- The point 'A' corresponds to the unloaded condition.
- The point 'B' corresponds to the nominal yield strength and yield rotation θ_y.
- The point 'C' corresponds to the ultimate strength and ultimate rotation θ_u, following which failure takes place.
- The point 'D' corresponds to the residual strength, if any, in the member. It is usually limited to 20% of the yield strength, and ultimate rotation, θ_u can be taken with that.
- The point 'E' defines the maximum deformation capacity and is taken as $15\theta_y$ or θ_u, whichever is greater.

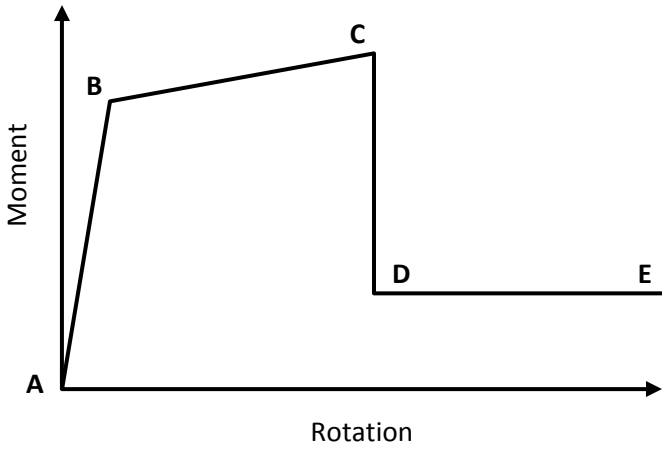

Fig.5.14. Idealised moment-rotation curve of RC elements

While applying Eqs.5.9 and 5.10 to determine the ultimate and yield rotations, care must be taken to adopt the correct value of the length *l*, applicable for cantilever action. In the case of a frame member in a multi-storey frame subject to lateral loads, it may be conveniently assumed that the points of contra flexure are located (approximately) at the mid-points of the beams and columns. In such cases, an approximate value of *l* is given by half the span of the member under consideration.

5.5. MODELLING OF SHEAR HINGES

When there is no prior failure in shear, flexural plastic hinges will develop along with the predicted values of ultimate moment capacity. Design codes prescribe specifications (e.g. ductile detailing requirement of IS 13920: 1993) for adequate shear reinforcement, corresponding to the ultimate moment capacity level. Therefore, it is obvious for a code designed building to fail in flexure and not in shear. There are a lot of buildings existing those are not detailed with IS 13920: 1993. Also, poor construction practise may lead to shear failure in framed building in the event of severe earthquakes.

Shear failure mostly occur in beams and columns owing to inadequate shear design. In non-linear analysis, this can be modelled by providing 'shear hinges'. These hinges located at the same points as the flexural hinges near the beam column joints. If the shear hinge mechanism occurred before the formation of flexural hinge, the moment demand gets automatically restricted because of this flexural hinge may not develop.

In this section, procedure for generating shear force-deformation curves to assign shear hinges for beams and columns explained. It is assumed that shear force-deformation curves is symmetric for positive and negative shear forces. Figure 5.15 represents typical

force deformations curve. In case of column, yield shear strength (V_y) is calculated by adding strength of the shear reinforcement (V_{sy}) to the shear strength of the concrete section (V_c). But in case of beam for medium and high ductility, shear strength contribution of concrete is completely ignored as in cracked section concrete does not provide any shear resistance. As per clause 40.4 of IS 456: 2000, Shear resistance carried by shear reinforcement (V_{sy}) is

$$V_s = 0.87 f_y A_{sv} \frac{d}{s_v} \qquad (5.13)$$

Where f_y = Yield stress of transverse reinforcement.

A_{sv} = Total cross sectional area of one stirrup considering all legs.

d = Effective depth.

S_v = Spacing between two stirrups.

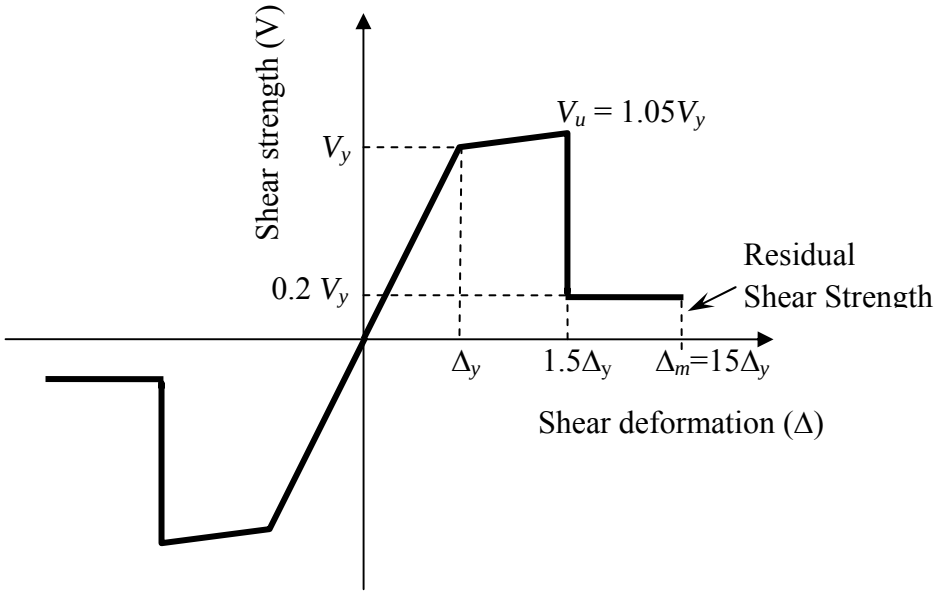

Fig.5.15. Typical shear force-deformation curves to model shear hinges (IITM-SERC Report, 2005)

In the actual strain hardened reinforcement for calculations of V_{sy} above formula is used putting f_y instead of $0.87f_y$.

$$V_s = 1.0\, f_y A_{sv} \frac{d}{s_v} \qquad (5.14)$$

In case of column shear strength in existing construction is calculated by the following expression

$$V_u = V_c + V_s \qquad (5.15)$$

As per clause 40.2.2 of IS 456:2000 shear resistance carried by concrete V_c is

$$V_c = \delta \tau_c b d \qquad (5.16)$$

The factor δ is defined in Chapter 2 (Eq. 2.2)

As per ATC 40, for moderate and high ductile column sections

$$\delta = 0 + \frac{3P_u}{A_g\ f_{ck}} \leq 0.5 \qquad (5.17)$$

Shear deformation (Δ) is to be calculated by

$$\Delta = \frac{yield\ shear\ strength}{shear\ stiffness} = \frac{R}{K_v} \qquad (5.18)$$

As shown in Equation 5.19, yield deformation should be calculated using shear stiffness of un-cracked member

$$K_v = \frac{1}{f}\left(\frac{G b_w d}{l}\right) \qquad (5.19)$$

Where G = Shear modulus of the reinforced concrete section, $A_g = b_w d$ = Gross area of the section and l = Length of member

f is factor to account non-uniform distribution of shear stress. For rectangular section, f is equal to 1.2 and for T and I section f is equal to 1.0.

By using shear stiffness of the cracked member, ultimate shear deformation can be calculated. Using the procedure explained Park and Paulay (1975), shear stiffness for the cracked member can be calculated.

Shear stiffness of a rectangular section with 45^0 diagonal cracks and vertical stirrups is given by

$$K_{v,45} = \left(\frac{\rho_v}{1 + 4n\rho_v} \right) E_s b_w d \qquad (5.20)$$

For other inclination of cracking and stirrups, similar expression is available in Park and Paulay (1975).

As per FEMA recommendations, for modelling of the shear hinges as shown in Figure 5.9 the ultimate shear strength (V_u) is taken as 5% more than yield shear strength (V_y) and residual shear strength is taken as 20% of the yield shear strength. Similarly maximum shear deformation (Δ_m) is considered as 15 times the yield deformation (Δ_y).

In this study, shear strength was calculated by using IS code 456: 2000 and shear displacement at yield and ultimate point were calculated by using Priestley et al. (1996) and Park and Paulay (1975) model respectively.

5.6. SUMMARY

This chapter starts with basic modelling technique for the linear and nonlinear analyses of the selected framed building. Then modelling nonlinear point plastic flexure and shear hinges for RC rectangular section is explained. This chapter also describes the geometries, frame section details including the reinforcement detail, foundation detail of the selected building choose in the present study.

CHAPTER 6

NONLINEAR STATIC (PUSHOVER) ANALYSIS

6.1. INRODUCTION

A nonlinear pushover analysis of the selected building is carried out as per FEMA 356 for evaluating the structural seismic response. In this analysis gravity loads and a representative lateral load pattern are applied to frame structure. The lateral loads were applied monotonically in a step-by-step manner. The applied lateral loads in X- direction representing the forces that would be experienced by the structures when subjected to ground shaking. The applied lateral forces were the product of mass and the first mode shape amplitude at each story level under consideration. P–Delta effects were also considered in account. At each stage, structural elements experience a stiffness change as shown in Fig. 6.1, where IO, LS and CP stand for immediate occupancy, life safety and collapse prevention respectively.

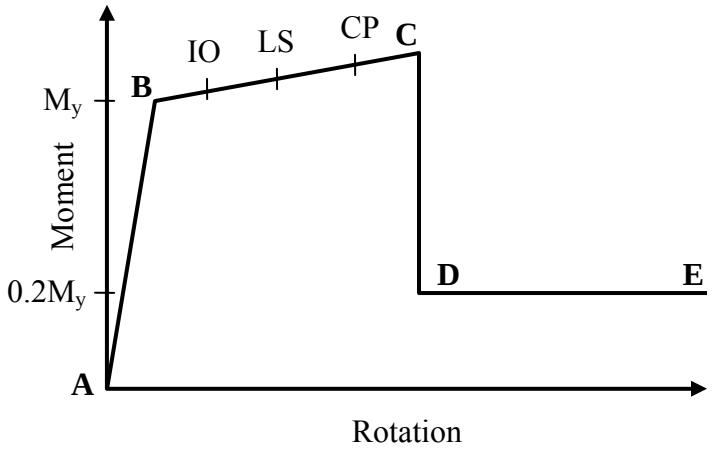

Fig.6.1. Load –Deformation curve

Refer Annexure B for details of the pushover analysis procedures. First total gravity load (Dead load and 25% live load) is applied in a load controlled pushover analysis followed by lateral load pushover analyses using displacement control. An invariant parabolic load pattern similar to IS 1893:2002 equivalent static analyses is considered for all the pushover analyses carried out here. This chapter presents the results obtained from the pushover analyses and discusses the nonlinear behaviour of the two selected buildings with and without shear hinges respectively.

6.2. CAPACITY CURVE

In pushover analysis, the behaviour of the structure is depends upon the capacity curve that represents the relationship between the base shear force and the roof displacement. Due to this convenient representation in practice engineer can be visualized easily. It is observed that roof displacement was used for the capacity curve because it is widely accepted in practice. Two models of the selected building one with shear hinges and other without shear hinges are analysed in the present study.

1. Considering Flexural Hinges only.
2. Considering both Flexural and Shear Hinges

6.2.1. Shear Hinge Properties for the Frame Elements

Shear hinge properties for individual beams and columns are calculated as per the procedure given in Chapter 5 (Section 5.5). Tables 6.1 and 6.2 present the calculated shear hinge properties for beam and column sections respectively. Shear hinges for beams are modelled in one vertical direction (V2) whereas for columns shear hinges are modelled in two orthogonal horizontal directions (V2 and V3)

Table 6.1. Details of the calculated shear hinge properties of beams

Plinth, Ground, First and Second floor beam								
Beam ID	Yield Force (kN)	Yield Disp (mm)	Ultimate Force (kN)	Ultimate Disp (mm)	Residual Force (kN)	Plastic Disp (mm)	Member Length (mm)	Disp Ductility (μ)
FB1A	63.90	2.48	67.1	2.84	12.78	0.36	2890	0.012
FB1B	63.90	2.42	67.1	2.76	12.78	0.34	2810	0.012
FB2A	63.90	2.45	67.1	2.8	12.78	0.35	2855	0.012
FB2B	63.90	2.39	67.1	2.73	12.78	0.34	2775	0.012
FB2C	63.90	1.16	67.1	1.33	12.78	0.17	1350	0.013
FB4	63.90	1.92	67.1	2.19	12.78	0.27	2230	0.012
FB5	63.90	1.85	67.1	2.11	12.78	0.26	2150	0.012
FB6A	63.90	2.11	67.1	2.41	12.78	0.3	2450	0.012
FB6B	63.90	2.04	67.1	2.33	12.78	0.29	2375	0.012
FB6C	63.90	2.04	67.1	2.33	12.78	0.29	2375	0.012
FB6D	63.90	2.11	67.1	2.41	12.78	0.3	2450	0.012
FB10A	63.90	1.9	67.1	2.17	12.78	0.27	2205	0.012
FB10B	63.90	0.59	67.1	0.67	12.78	0.08	685	0.012
FB11	63.90	2.48	67.1	2.83	12.78	0.35	2885	0.012
FB12A	63.90	0.74	67.1	0.84	12.78	0.1	860	0.012
FB12B	63.90	1.83	67.1	2.09	12.78	0.26	2130	0.012
FB13	63.90	2.43	67.1	2.77	12.78	0.34	2825	0.012
FB14	63.90	1.34	67.1	1.53	12.78	0.19	1556	0.012
FB15	63.90	0.99	67.1	1.13	12.78	0.14	1150	0.012
FB16	63.90	1.29	67.1	1.48	12.78	0.19	1506	0.013
FB 17	63.90	2.84	67.1	3.24	12.78	0.4	3300	0.012
FB7	63.90	1.65	67.1	1.89	12.78	0.24	1925	0.012
FB8A	63.90	2.36	67.1	2.7	12.78	0.34	2750	0.012
FB8B	63.90	1.83	67.1	2.09	12.78	0.26	2130	0.012
FB9	63.90	1.95	67.1	2.22	12.78	0.27	2265	0.012
MB2	119.81	1.72	125.8	1.92	23.96	0.2	2000	0.010

Table 6.1. (contd.) Details of the calculated shear hinge properties of beams

Roof floor beam								
Beam ID	Yield Force (kN)	Yield Disp (mm)	Ultimate Force (kN)	Ultimate Disp (mm)	Residual Force (kN)	Plastic Disp (mm)	Member Length (mm)	Disp Ductility (μ)
RB1A	63.90	2.48	67.1	2.84	12.78	0.36	2890	0.012
RB1B	63.90	2.42	67.1	2.76	12.78	0.34	2810	0.012
RB2A	63.90	2.45	67.1	2.8	12.78	0.35	2855	0.012
RB2B	63.90	2.39	67.1	2.73	12.78	0.34	2775	0.012
RB2C	63.90	1.16	67.1	1.33	12.78	0.17	1350	0.013
RB4	63.90	1.92	67.1	2.19	12.78	0.27	2230	0.012
RB5	63.90	1.85	67.1	2.11	12.78	0.26	2150	0.012
RB6A	63.90	2.11	67.1	2.41	12.78	0.3	2450	0.012
RB6B	63.90	2.04	67.1	2.33	12.78	0.29	2375	0.012
RB6C	63.90	2.04	67.1	2.33	12.78	0.29	2375	0.012
RB6D	63.90	2.11	67.1	2.41	12.78	0.3	2450	0.012
RB8A	63.90	2.36	67.1	2.7	12.78	0.34	2750	0.012
RB8B	63.90	1.83	67.1	2.09	12.78	0.26	2130	0.012
RB10A	63.90	1.9	67.1	2.17	12.78	0.27	2205	0.012
RB10B	63.90	0.59	67.1	0.67	12.78	0.08	685	0.012
RB11	63.90	2.48	67.1	2.83	12.78	0.35	2885	0.012
RB12A	63.90	0.74	67.1	0.84	12.78	0.1	860	0.012
RB12B	63.90	1.83	67.1	2.09	12.78	0.26	2130	0.012
RB13	63.90	2.43	67.1	2.77	12.78	0.34	2825	0.012
RB14	63.90	1.34	67.1	1.53	12.78	0.19	1556	0.012
RB15	63.90	0.99	67.1	1.13	12.78	0.14	1150	0.012
RB16	63.90	1.29	67.1	1.48	12.78	0.19	1506	0.013
RB17	63.90	2.84	67.1	3.24	12.78	0.4	3300	0.012
RB7	63.90	1.65	67.1	1.89	12.78	0.24	1925	0.012

Table 6.2. Details of the calculated shear hinge properties of column

Ground floor column (Column Shear V_2) of 4.08m height							
Column ID	Yield Force (kN)	Yield Disp (mm)	Ultimate Force (kN)	Ultimate Disp (mm)	Residual Force (kN)	Plastic Disp (mm)	Disp Ductility (μV2)
A1	43.81	5.24	46.0	10.85	8.76	5.61	0.19
A11	36.19	5.17	38.0	10.85	7.24	5.68	0.19
A8	35.62	5.17	37.4	10.85	7.12	5.68	0.19
B1	54.29	5.17	57.0	10.86	10.86	5.69	0.19
B10	131.52	5.28	138.1	8.914	26.30	3.64	0.12
B101	113.81	5.17	119.5	8.914	22.76	3.74	0.12
B12	123.33	5.23	129.5	8.914	24.67	3.69	0.12
B121	112.57	5.16	118.2	8.914	22.51	3.75	0.13
B14	48.86	5.29	51.3	10.85	9.77	5.56	0.19
B141	36.86	5.18	38.7	10.85	7.37	5.67	0.19
B4	79.05	5.18	83.0	8.38	15.81	3.20	0.11
B8	44.76	5.25	47.0	10.85	8.95	5.60	0.19
B81	35.43	5.17	37.2	10.85	7.09	5.68	0.19
C12	45.62	5.26	47.9	10.85	9.12	5.59	0.19
C121	35.90	5.17	37.7	10.85	7.18	5.68	0.19
E11	64.00	5.17	67.2	8.8	12.80	3.63	0.12
H11	43.33	5.24	45.5	10.85	8.67	5.61	0.19
H111	35.90	5.17	37.7	10.85	7.18	5.68	0.19

Table 6.2. (contd.) Details of the calculated shear hinge properties of column

Ground floor column (Column Shear V_3) of 4.08m height							
Column ID	Yield Force (kN)	Yield Disp (mm)	Ultimate Force (kN)	Ultimate Disp (mm)	Residual Force (kN)	Plastic Disp (mm)	Disp Ductility (μV3)
A1	61.05	5.26	64.1	11.75	12.21	6.49	0.22
A11	53.43	5.18	56.1	11.75	10.69	6.57	0.22
A8	35.62	5.17	37.4	10.85	7.12	5.68	0.19
B1	64.38	5.17	67.6	8.8	12.88	3.63	0.12
B10	53.05	5.18	55.7	9.71	10.61	4.53	0.15
B101	36.48	5.16	38.3	9.71	7.30	4.55	0.15
B12	45.05	5.17	47.3	9.71	9.01	4.54	0.15
B121	35.24	5.32	37.0	9.71	7.05	4.39	0.15
B14	66.10	5.18	69.4	11.75	13.22	6.57	0.22
B141	54.10	5.17	56.8	11.75	10.82	6.58	0.22
B4	56.10	5.17	58.9	10.35	11.22	5.18	0.17
B8	62.10	5.28	65.2	11.75	12.42	6.47	0.22
B81	35.43	5.17	37.2	10.85	7.09	5.68	0.19
C12	62.86	5.27	66.0	11.75	12.57	6.48	0.22
C121	35.90	5.17	37.7	10.85	7.18	5.68	0.19
E11	53.90	5.17	56.6	10.67	10.78	5.50	0.18
H11	43.33	5.24	45.5	10.85	8.67	5.61	0.19
H111	35.90	5.17	37.7	10.85	7.18	5.68	0.19

Table 6.2. (contd.) Details of the calculated shear hinge properties of column

First, Second and Third Floor columns (Column Shear V_2) of 3.00m height							
Column ID	Yield Force (kN)	Yield Disp (mm)	Ultimate Force (kN)	Ultimate Disp (mm)	Residual Force (kN)	Plastic Disp (mm)	Disp Ductility (μV2)
A1	43.81	7.13	46	14.76	8.76	7.63	0.19
A11	36.19	7.03	38	14.76	7.24	7.73	0.19
A8	35.62	7.02	37.4	14.76	7.12	7.74	0.19
B1	54.29	7.03	57.0	14.5	10.86	7.47	0.18
B10	131.52	7.18	138.1	12.12	26.30	4.94	0.12
B101	113.81	7.03	119.5	12.12	22.76	5.09	0.12
B12	123.33	7.1	129.5	12.12	24.67	5.02	0.12
B121	112.57	7.02	118.2	12.12	22.51	5.10	0.13
B14	48.86	7.19	51.3	14.76	9.77	7.57	0.19
B141	36.86	7.04	38.7	14.76	7.37	7.72	0.19
B4	79.05	7.04	83.0	11.34	15.81	4.30	0.11
B8	44.76	7.14	47.0	14.76	8.95	7.62	0.19
B81	35.43	7.02	37.2	14.76	7.09	7.74	0.19
C12	45.62	7.15	47.9	14.76	9.12	7.61	0.19
C121	35.90	7.03	37.7	14.76	7.18	7.73	0.19
E11	64.00	7.03	67.2	11.98	12.80	4.95	0.12
H11	43.33	7.12	45.5	14.76	8.67	7.64	0.19
H111	35.90	7.03	37.7	14.76	7.18	7.73	0.19

Table 6.2. (contd.) Details of the calculated shear hinge properties of column

First, Second and Third Floor column (Column Shear V_3) of 3.00m height							
Column ID	Yield Force (kN)	Yield Disp (mm)	Ultimate Force (kN)	Ultimate Disp (mm)	Residual Force (kN)	Plastic Disp (mm)	Disp Ductility (μV3)
A1	61.05	7.16	64.1	15.98	12.21	8.82	0.22
A11	53.43	7.04	56.1	15.98	10.69	8.94	0.22
A8	35.62	7.03	37.4	14.76	7.12	7.73	0.19
B1	64.38	7.03	67.6	11.98	12.88	4.95	0.12
B10	53.05	7.04	55.7	13.21	10.61	6.17	0.15
B101	36.48	7.02	38.3	13.21	7.30	6.19	0.15
B12	45.05	7.03	47.3	13.21	9.01	6.18	0.15
B121	35.24	7.01	37.0	13.21	7.05	6.20	0.15
B14	66.10	7.24	69.4	15.98	13.22	8.74	0.21
B141	54.10	7.05	56.8	15.98	10.82	8.93	0.22
B4	56.10	7.03	58.9	14.07	11.22	7.04	0.17
B8	62.10	7.18	65.2	15.98	12.42	8.80	0.22
B81	35.43	7.02	37.2	14.76	7.09	7.74	0.19
C12	62.86	7.19	66.0	15.98	12.57	8.79	0.22
C121	35.90	7.03	37.7	14.76	7.18	7.73	0.19
E11	53.90	7.03	56.6	14.5	10.78	7.47	0.18
H11	43.33	7.12	45.5	14.76	8.67	7.64	0.19
H111	35.90	7.03	37.7	14.76	7.18	7.73	0.19

6.2.2. Capacity Curves for Push X and for Push Y

The two resulting capacity curves for Push X and for Push Y analysis are plotted in Figs. 6.2 and 6.3, respectively. Two building models with and without shear are considered. They are initially linear but start to deviate from linearity as the beams and the columns undergo inelastic deformation. When

the buildings are pushed well into the inelastic range, the curves become linear again but with a smaller slope. The two curves could be approximated by a bilinear relationship. Tables 6.3 and 6.4 presents the numerical data for capacity curves obtained from pushover analysis in X- and Y-directions respectively

Table 6.3. Details of the Capacity Curves obtained from Push-X Analysis

	With Shear Hinge		Without Shear Hinge	
Step	Base Shear (kN)	Roof Displ. (m)	Base Shear (kN)	Roof Displ. (m)
0	0	0	0	0
1	192.4	0.0071	192.6	0.0070
2	356.7	0.0133	757.5	0.0322
3	351.9	0.0133	907.4	0.0455
4	492.3	0.0190	973.4	0.0578
5	487.8	0.0190	1098.0	0.1165
6	533.1	0.0210	1167.9	0.1701
7	532.1	0.0210	1183.0	0.1701
8	625.9	0.0256	1194.1	0.1765
9	620.7	0.0256	766.4	0.1144
10	644.7	0.0268		
11	637.8	0.0268		
12	710.3	0.0311		
13	704.2	0.0311		
14	706.1	0.0312		
15	639.3	0.0312		
16	684.7	0.0346		
17	667.6	0.0346		
18	670.5	0.0348		
19	617.2	0.0337		

Table 6.4. Details of the Capacity Curves obtained from Push-Y Analysis

	With Shear Hinge		Without Shear Hinge	
Step	Base Shear (kN)	Roof Displ. (m)	Base Shear (kN)	Roof Displ. (m)
0	0	0	0	0
1	192.2	0.0018	192.2	0.0017
2	513.6	0.0057	531.9	0.0058
3	504.8	0.0057	765.3	0.0126
4	553.5	0.0067	983.4	0.0270
5	551.4	0.0067	981.1	0.0270
6	551.9	0.0067	983.2	0.0271
7	544.6	0.0067	962.7	0.0271
8	599.6	0.0084	964.7	0.0272
9	594.6	0.0084	976.0	0.0276
10	611.9	0.0089	978.2	0.0278
11	593.1	0.0089	980.0	0.0278
12	632.9	0.0102	980.9	0.0278
13	630.0	0.0103	984.3	0.0279
14	657.9	0.0115	966.6	0.0278
15	645.3	0.0115		
16	654.5	0.0117		
17	674.5	0.0127		
18	654.3	0.0128		
19	660.1	0.0130		

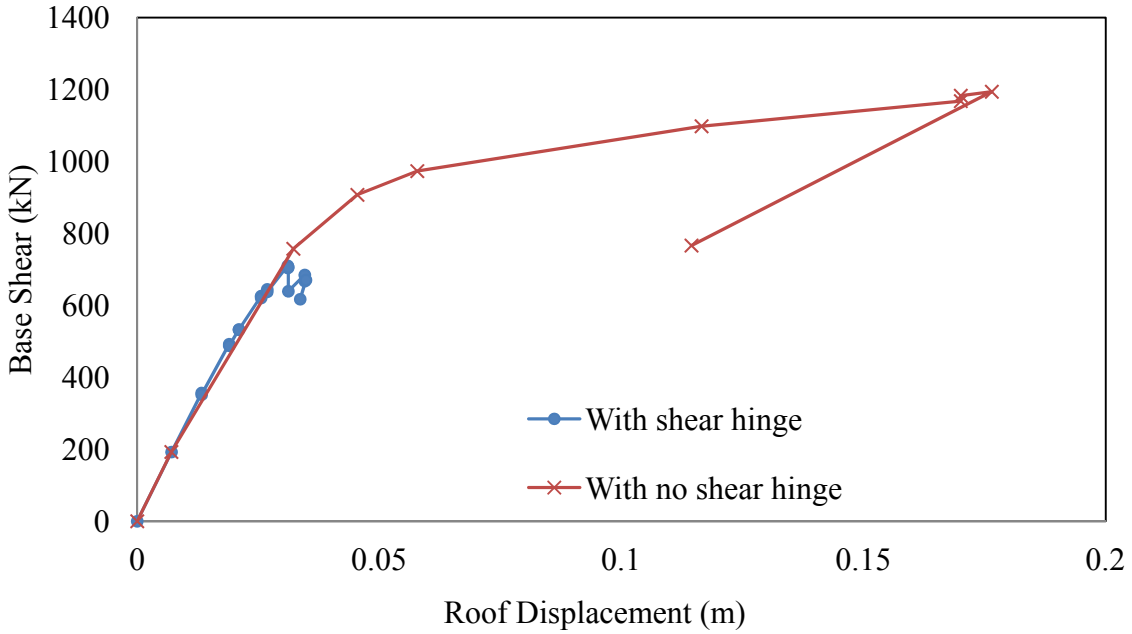

Fig. 6.2. Capacity curve for Push X analysis

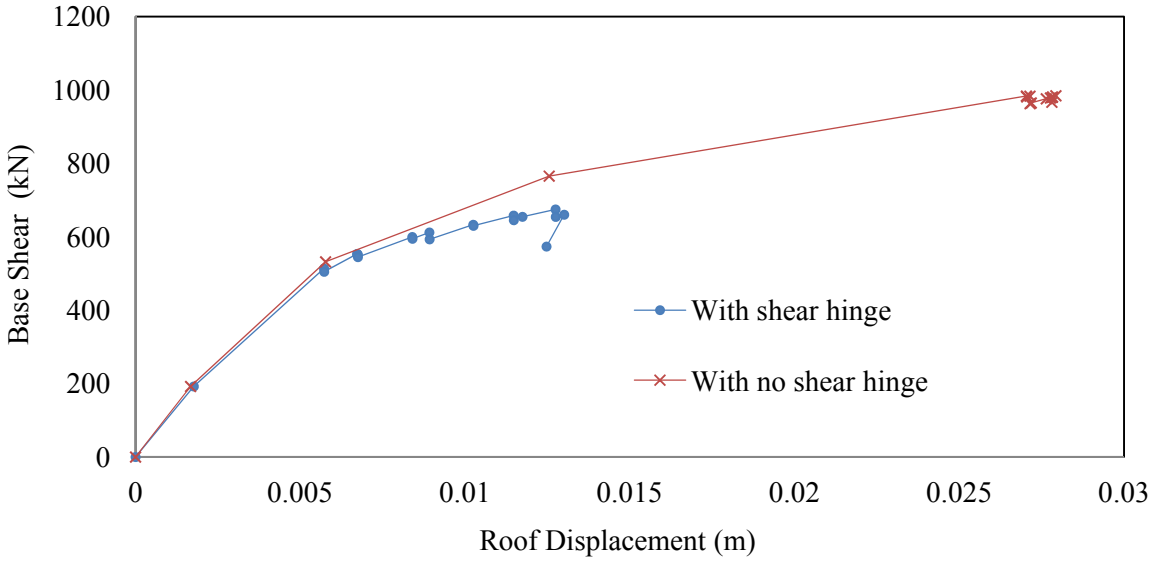

Fig. 6.3. Capacity curve for Push Y analysis

Table 6.5 presents the summary of the base shear and roof displacement capacity of the building as obtained from pushover analysis. Figs. 6.2 and 6.3 together with Table 6.5 clearly show how the pushover analysis overestimates the base shear and roof displacement capacity of the building when shear failure mode is not considered in the analysis. As per Table 6.5 pushover analysis overestimates base shear capacity of the building by approximately 70% in X-direction and 45% in Y-direction when shear hinges ignored. The maximum roof displacement capacity is overestimated by 460% in X-direction and 120% in Y-direction.

Table 6.5. Summary of the base shear and roof displacement capacity of the building

	Capacity (kN)	Displacement (mm)
Push -X analysis		
With shear hinge	711	31.2
With no shear hinge	1195	176.5
Push -Y analysis		
With shear hinge	675	12.7
With no shear hinge	985	27.8

6.2.3. Ductility ratio for Push X and Push Y analysis

Table 6.6 presents the numerical values for estimated yield, ultimate and plastic displacement of the building in global sense. This table also shows the ductility ratio (ratio between ultimate and yield displacement) estimated for different analysis case. These data are derived from the capacity curves of the building. It is found from the table that shear failure makes a structure less ductile. In X-direction, ductility ratio reduces from 5.5 to 1.1 when shear hinges are incorporated in the model. Similarly, ductility ratio reduces from 4.7 to 2.2 in Y-direction.

Table 6.6. Global ductility ratio of the building in two directions

	Push-X		Push-Y	
	No shear	With shear	No shear	With shear
Yield Disp (mm)	32.2	31.1	5.8	5.7
Ultimate Disp (mm)	176.5	34.8	27.0	17.7
Plastic Disp (mm)	144.3	3.7	21.2	7.0
Ductility ratio	5.5	1.1	4.7	2.2

6.3. PLASTIC HINGE MECHANISM

Sequences of plastic hinge formation are presented in Figs. 6.4 to 6.7. Performance levels of the plastic hinges are shown using colour code. The global yielding point corresponds to the displacement on the capacity curve where the system starts to soften. The ultimate point is considered at a displacement when lateral load capacity suddenly drops. Plastic hinges formation first occurs in beam ends and columns of lower stories, then extended to upper stories and continue with yielding of interior intermediate columns.

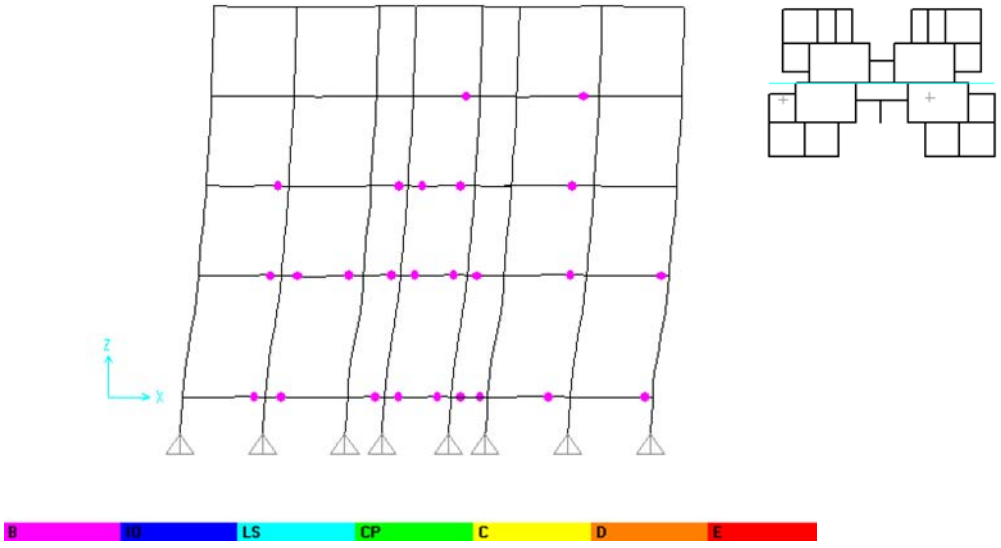

(a) At Step# 2 (757.5 kN, 32.2 mm)

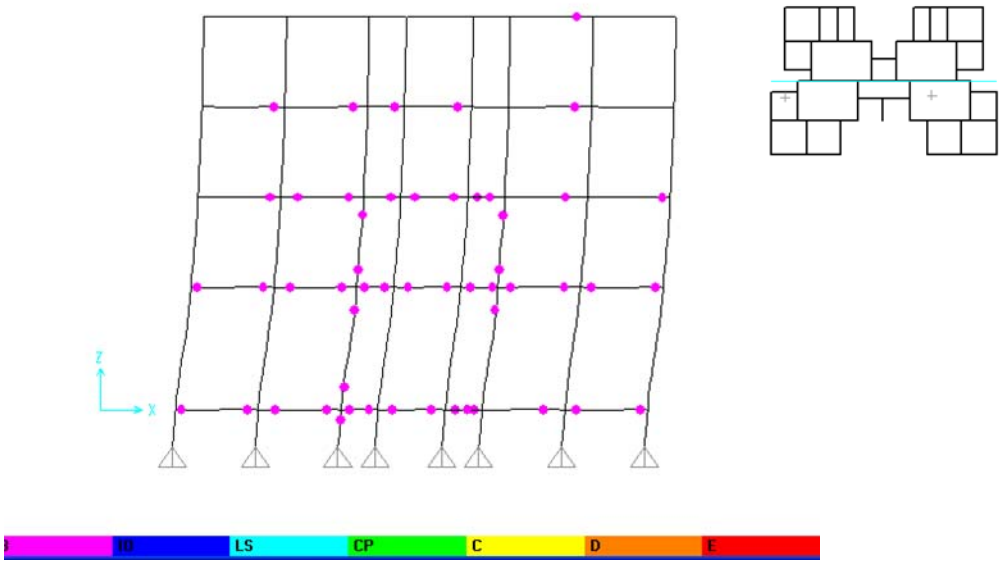

(b) At Step# 4 (973.4 kN, 57.8 mm)

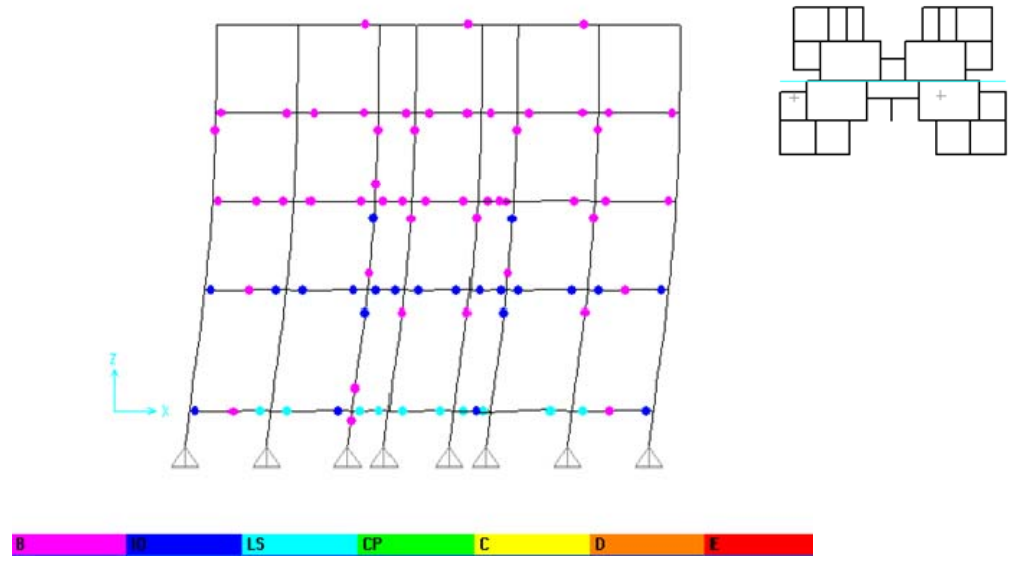

(c) At Step# 8 (1194.1 kN, 176.5 mm)

Fig. 6.4. Sequence of yielding for building without shear hinge (Push-X)

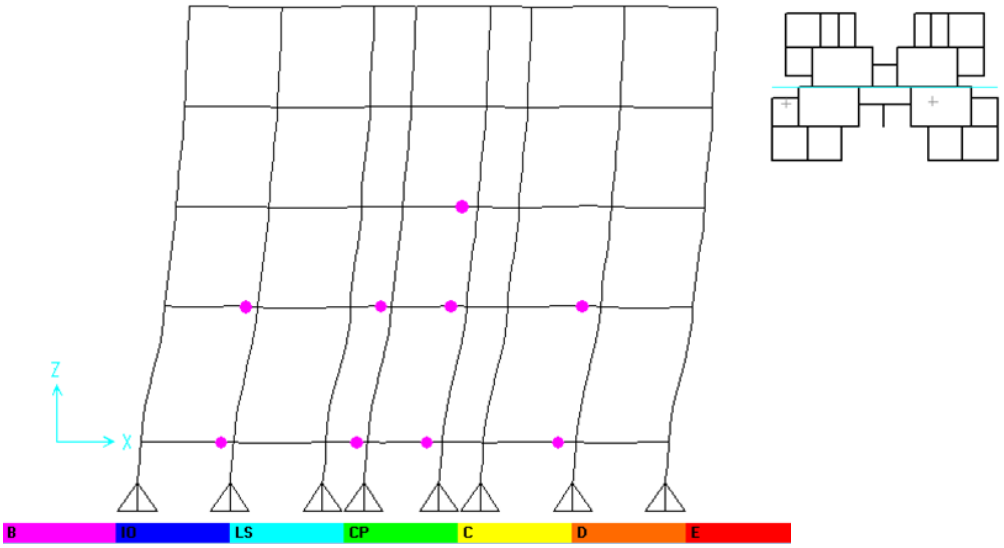

(a) At Step# 4 (492.3 kN, 19.0 mm)

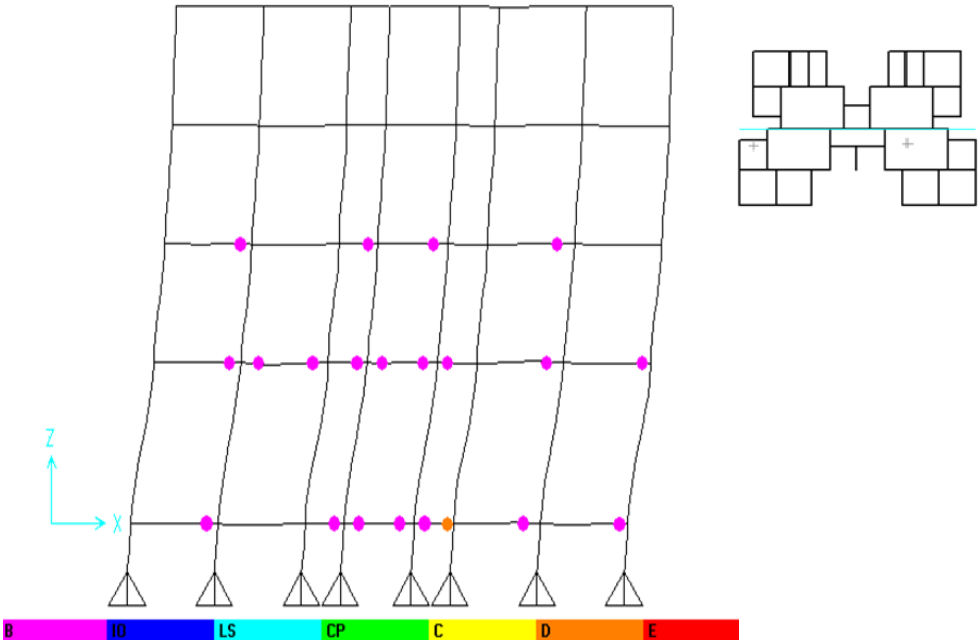

(b) At Step# 12 (710.3 kN, 31.1 mm)

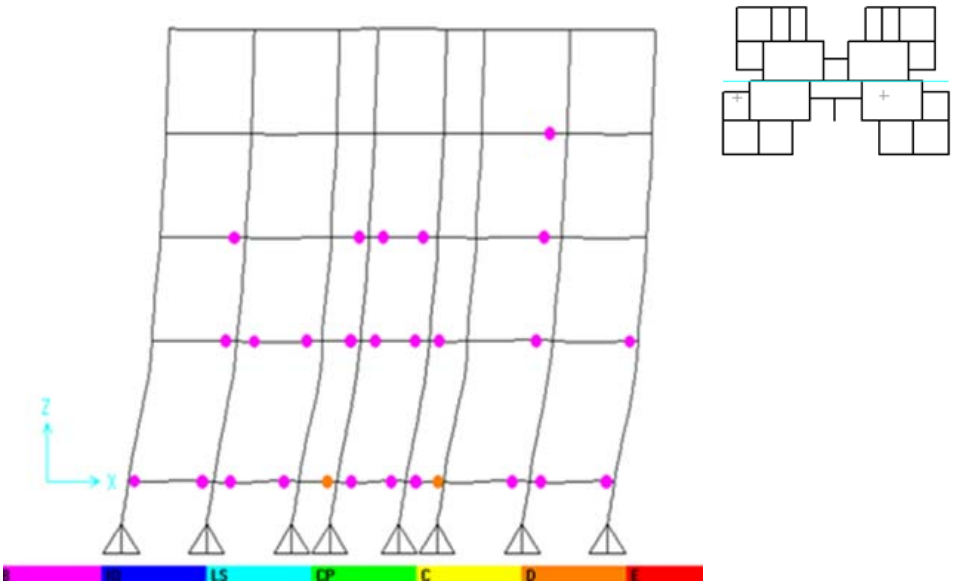

(c) At Step# 19 (617.2 kN, 33.7 mm)

Fig. 6.5. Sequence of yielding for building with shear hinge (Push-X)

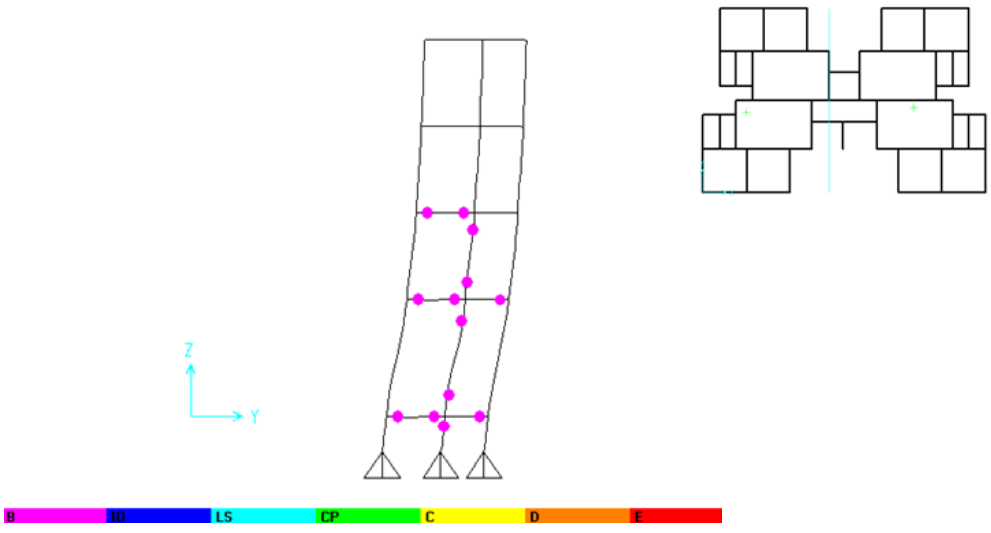

(a) At Step# 3 (765.3kN, 12.6 mm)

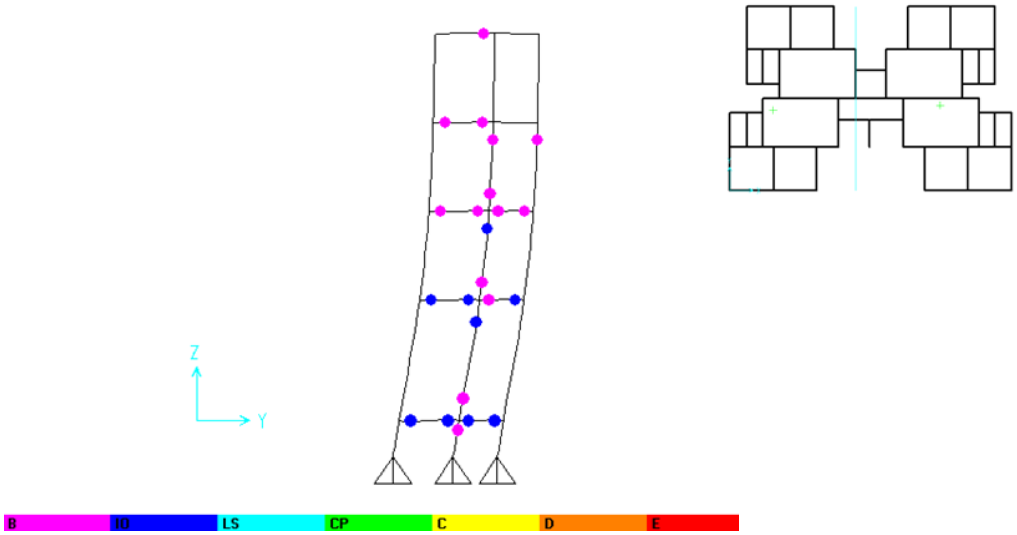

(b) At Step# 7 (962.7 kN, 27.1 mm)

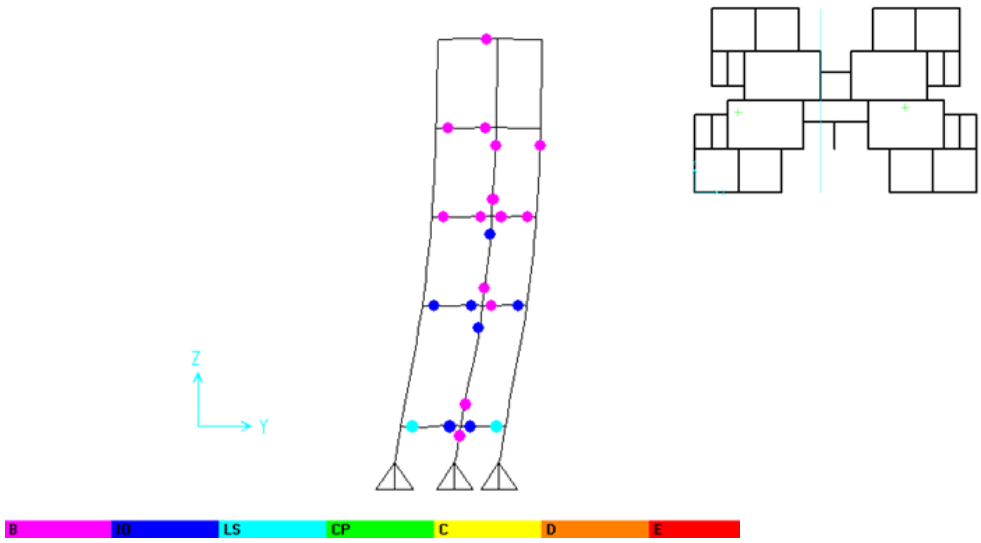

(c) At Step# 14 (966.6 kN, 27.8 mm)

Fig. 6.6. Sequence of yielding for building without shear hinge (Push-Y)

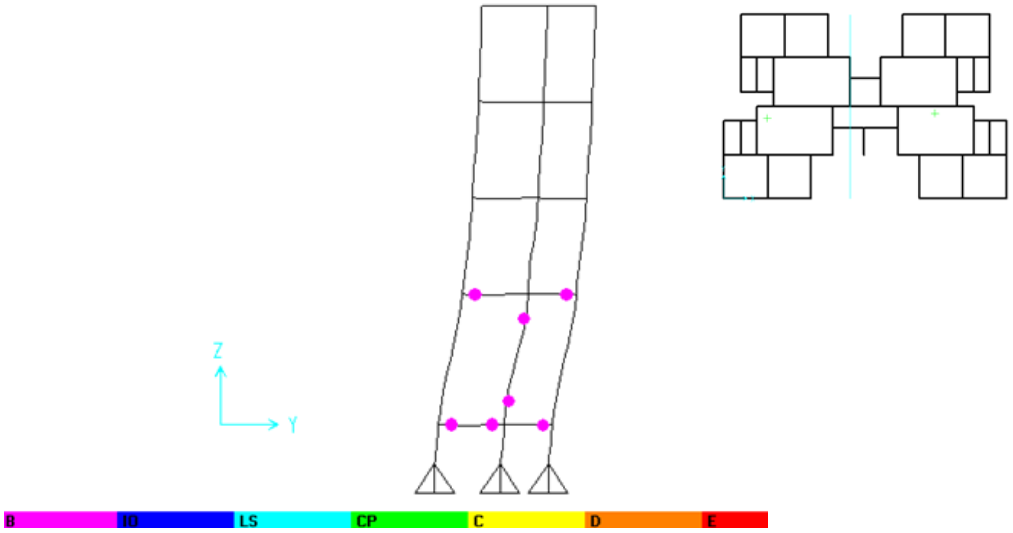

(a) At Step# 11 (593.1 kN, 8.9 mm)

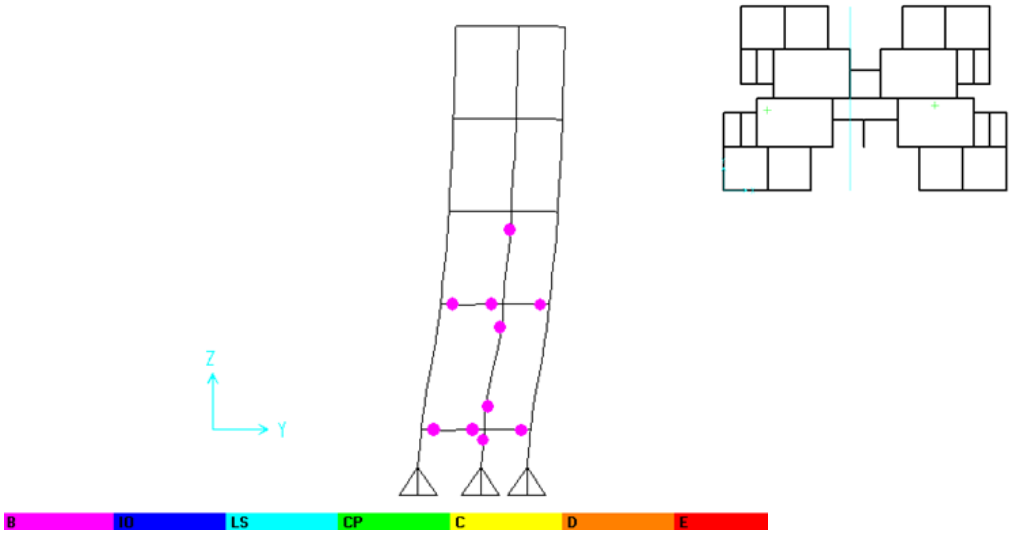

(b) At Step# 15 (645.3 kN, 11.5 mm)

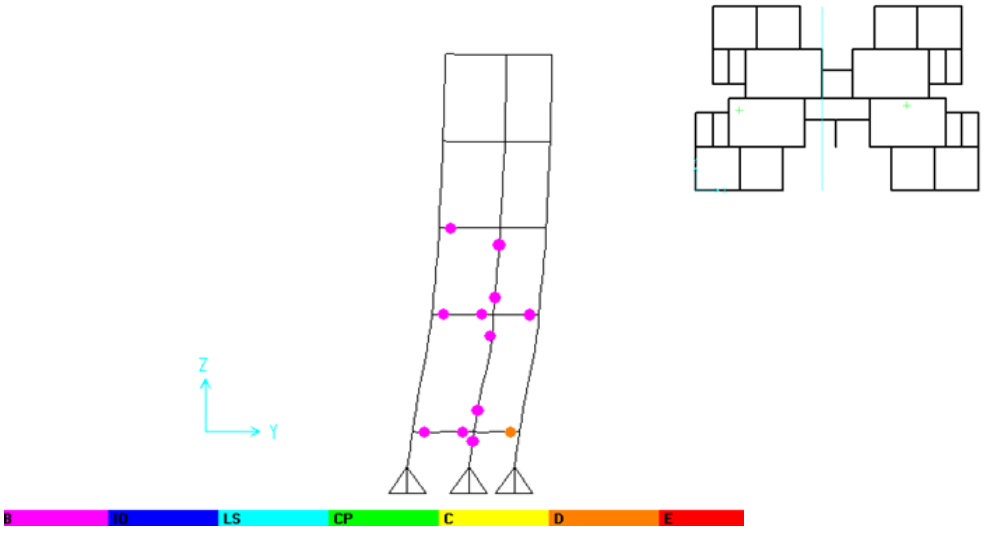

(c) At Step# 19 (660.1 kN, 13.0 mm)

Fig. 6.7. Sequence of yielding for building with shear hinge (Push-Y)

6.4. SUMMARY

This chapter presents the results obtained from pushover analysis of the selected building modes. Analyses were carried out for two building models, one without shear hinges and other with shear hinges, and for two orthogonal lateral directions (X- and Y-) of each model. The results presented here shows that the analysis can grossly overestimate the base shear and maximum roof displacement capacity of a building if the model ignores shear hinges. Also, estimated ductility ratio is found to be very high for the selected building model that does not consider shear hinge. These results demonstrate the importance of shear hinge in as seismic evaluation problem.

CHAPTER 7

SUMMARY AND CONCLUSIONS

7.1. SUMMARY

The main objective of the present study is to demonstrate the importance of shear hinges in seismic evaluation of RC framed building. A detailed literature review is carried out as part of the present study on shear strength and displacement capacity of rectangular RC sections and seismic evaluation based on nonlinear static pushover analysis. Different methods to estimate shear strength and displacement capacity are studied. These calculation procedures are discussed through example calculations in Chapters 3 and 4.

There is no published literature found on the nonlinear force-deformation model of RC rectangular section for shear. A model for nonlinear shear force versus shear deformation relation is developed using FEMA 356, IS 456:2000, Priestley et al. (1996) and Park and Paulay (1975). To demonstrate the importance of shear hinges in seismic evaluation of RC framed building an existing framed residential apartment building is selected. This building is analyzed for two different cases: (a) considering flexural and shear hinges (b) considering only flexural hinges (*i.e.*, without considering shear hinges). The structures are analyzed for pushover analysis in X and Y directions.

Beams and columns in the present study were modelled as frame elements with the centrelines joined at nodes using commercial software SAP2000 (v14). The rigid beam-column joints were modelled by using end offsets at the joints. The floor slabs were assumed to act as diaphragms, which ensure integral action of all the vertical lateral load-

resisting elements. The weight of the slab was distributed as triangular and trapezoidal load to the surrounding beams. M 20 grade of concrete and Fe 415 grade of reinforcing steel were used to design the building. The column end at foundation was considered as fixed for all the models in this study.

The flexural hinges in beams are modelled with uncoupled moment (M3) hinges whereas for column elements the flexural hinges are modelled with coupled P-M2-M3 properties based on the interaction of axial force and bi-axial bending moments at the hinge location.

All the building models were then analysed using non-linear static (pushover) analysis. At first, the pushover analysis is done for the gravity loads (DL+0.25LL) incrementally under load control. The lateral pushover analysis (in X- and Y-directions) was followed after the gravity pushover, under displacement control.

Pushover analysis results for two different cases, as mentioned earlier, compared to identify the importance of the shear hinges in seismic evaluation problem.

7.2. CONCLUSIONS

Followings are the salient conclusions from the present study:

Shear strength

i) FEMA-356 does not consider contribution of concrete in shear strength calculation for beam under earthquake loading for moderate to high ductility.

ii) Contribution of web reinforcement in shear strength given in IS-456: 2000 and ACI-318: 2008 represent ultimate strength.

iii) FEMA-356 consider ultimate shear strength carried by the web reinforcement (= strength of the beam) as 1.05 times the yield strength. But there is no engineering background for this consideration.

iv) No clarity is found in yield strength from the literature.

Shear displacement at yield

i) The model by Sezen (2002) is based on regression analysis of test data

ii) Model by Panagiotakos and Fardis (2001) is simple but it is reported to be overestimating the shear displacement.

iii) Model proposed by Gerin and Adebar (2004) is reported to be underestimating the shear displacements at yield.

iv) Priestley et al. (1996) is reported to be most effective for calculating shear displacement at yield for beams and columns.

Ultimate Shear displacement

i) Model of Park and Paulay (1975) is reported to be most effective in predicting the ultimate shear displacements for beams and columns.

ii) CEB (1985) is also reported to be effective in predicting the ultimate shear displacements of beam.

iii) Model by Gerin and Adebar (2004) is reported to be not suitable for predicting the ultimate shear displacements.

Case study

i) The case study presented here demonstrate the importance of modelling shear hinges to correctly evaluate strength and ductility of the building

ii) When analysis ignores shear failure model it overestimate base shear and roof displacement capacity of the building.

iii) Presence of shear hinge can correctly reveal the non-ductile failure mode of the building.

7.3. SCOPE FOR FUTURE WORK

i) The nonlinear shear hinge properties of rectangular RC sections developed here can be validated through experimental study.

ii) The present study considers only rectangular sections with rectangular links as web reinforcement. This study can be further extended to spiral web reinforcement in circular section.

ANNEXURE A

PUSHOVER ANALYSIS (FEMA-356, ATC-40)

A.1 INTRODUCTION

The use of the nonlinear static analysis (pushover analysis) came in to practice in 1970's but the potential of the pushover analysis has been recognized for last 10-15 years. This procedure is mainly used to estimate the strength and drift capacity of existing structure and the seismic demand for this structure subjected to selected earthquake. This procedure can be used for checking the adequacy of new structural design as well. The effectiveness of pushover analysis and its computational simplicity brought this procedure in to several seismic guidelines (ATC 40 and FEMA 356) and design codes (Euro code 8 and PCM 3274) in last few years.

Pushover analysis is defined as an analysis wherein a mathematical model directly incorporating the nonlinear load-deformation characteristics of individual components and elements of the building shall be subjected to monotonically increasing lateral loads representing inertia forces in an earthquake until a 'target displacement' is exceeded. Target displacement is the maximum displacement (elastic plus inelastic) of the building at roof expected under selected earthquake ground motion. Pushover analysis assesses the structural performance by estimating the force and deformation capacity and seismic demand using a nonlinear static analysis algorithm. The seismic demand parameters are global displacements (at roof or any other reference point), storey drifts, storey forces, and component deformation and component forces. The analysis accounts for

geometrical nonlinearity, material inelasticity and the redistribution of internal forces. Response characteristics that can be obtained from the pushover analysis are summarised as follows:

a) Estimates of force and displacement capacities of the structure. Sequence of the member yielding and the progress of the overall capacity curve.
b) Estimates of force (axial, shear and moment) demands on potentially brittle elements and deformation demands on ductile elements.
c) Estimates of global displacement demand, corresponding inter-storey drifts and damages on structural and non-structural elements expected under the earthquake ground motion considered.
d) Sequences of the failure of elements and the consequent effect on the overall structural stability.
e) Identification of the critical regions, where the inelastic deformations are expected to be high and identification of strength irregularities (in plan or in elevation) of the building.

Pushover analysis delivers all these benefits for an additional computational effort (modeling nonlinearity and change in analysis algorithm) over the linear static analysis. Step by step procedure of pushover analysis is discussed next.

A.1.1 Pushover Analysis Procedure

Pushover analysis is a static nonlinear procedure in which the magnitude of the lateral load is increased monotonically maintaining a predefined distribution pattern along the height of the building (Fig. A.1a). Building is displaced till the ‘control node’ reaches

'target displacement' or building collapses. The sequence of cracking, plastic hinging and failure of the structural components throughout the procedure is observed. The relation between base shear and control node displacement is plotted for all the pushover analysis (Fig. A.1b). Generation of base shear – control node displacement curve is single most important part of pushover analysis. This curve is conventionally called as pushover curve or capacity curve. The capacity curve is the basis of 'target displacement' estimation.

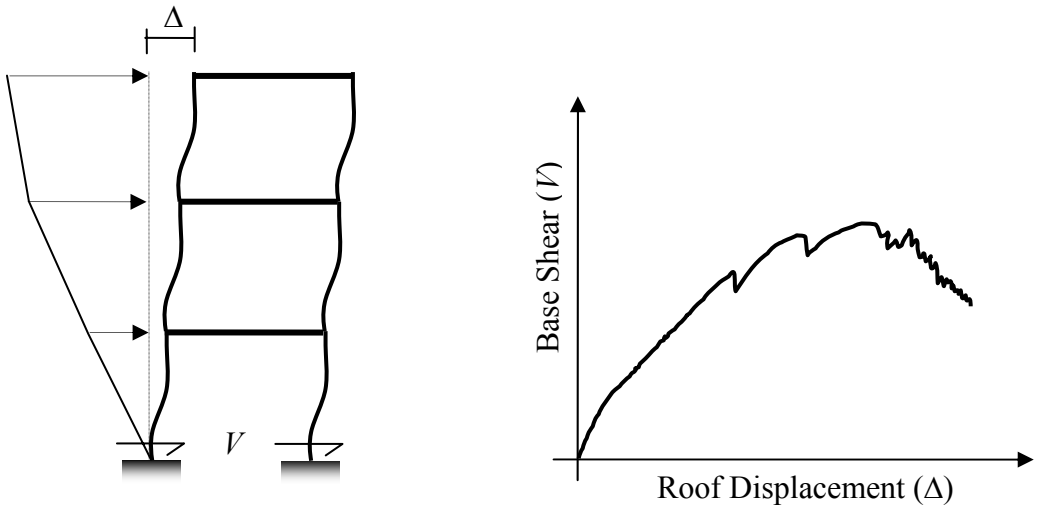

a) Building model b) Pushover curve

Fig. A.1: Schematic representation of pushover analysis procedure

So the pushover analysis may be carried out twice: (a) first time till the collapse of the building to estimate target displacement and (b) next time till the target displacement to estimate the seismic demand. The seismic demands for the selected earthquake (storey drifts, storey forces, and component deformation and forces) are calculated at the target displacement level. The seismic demand is then compared with the corresponding

structural capacity or predefined performance limit state to know what performance the structure will exhibit. Independent analysis along each of the two orthogonal principal axes of the building is permitted unless concurrent evaluation of bi-directional effects is required.

The analysis results are sensitive to the selection of the control node and selection of lateral load pattern. In general, the centre of mass location at the roof of the building is considered as control node. For selecting lateral load pattern in pushover analysis, a set of guidelines as per FEMA 356 is explained in Section A.1.2. The lateral load generally applied in both positive and negative directions in combination with gravity load (dead load and a portion of live load) to study the actual behavior.

A.1.2 Lateral Load Profile

In pushover analysis the building is pushed with a specific load distribution pattern along the height of the building. The magnitude of the total force is increased but the pattern of the loading remains same till the end of the process. Pushover analysis results (*i.e.*, pushover curve, sequence of member yielding, building capacity and seismic demand) are very sensitive to the load pattern. The lateral load patterns should approximate the inertial forces expected in the building during an earthquake. The distribution of lateral inertial forces determines relative magnitudes of shears, moments, and deformations within the structure. The distribution of these forces will vary continuously during earthquake response as the members yield and stiffness characteristics change. It also depends on the type and magnitude of earthquake ground motion. Although the inertia force distributions vary with the severity of the earthquake

and with time, FEMA 356 recommends primarily invariant load pattern for pushover analysis of framed buildings.

Several investigations (Mwafy and Elnashai, 2000; Gupta and Kunnath, 2000) have found that a triangular or trapezoidal shape of lateral load provide a better fit to dynamic analysis results at the elastic range but at large deformations the dynamic envelopes are closer to the uniformly distributed force pattern. Since the constant distribution methods are incapable of capturing such variations in characteristics of the structural behavior under earthquake loading, FEMA 356 suggests the use of at least two different patterns for all pushover analysis. Use of two lateral load patterns is intended to bind the range that may occur during actual dynamic response. FEMA 356 recommends selecting one load pattern from each of the following two groups:

A. Group – I:

i) Code-based vertical distribution of lateral forces used in equivalent static analysis (permitted only when more than 75% of the total mass participates in the fundamental mode in the direction under consideration).

ii) A vertical distribution proportional to the shape of the fundamental mode in the direction under consideration (permitted only when more than 75% of the total mass participates in this mode).

iii) A vertical distribution proportional to the story shear distribution calculated by combining modal responses from a response spectrum analysis of the building (sufficient number of modes to capture at least 90% of the total

building mass required to be considered). This distribution shall be used when the period of the fundamental mode exceeds 1.0 second.

2. Group – II:

i) A uniform distribution consisting of lateral forces at each level proportional to the total mass at each level.

ii) An adaptive load distribution that changes as the structure is displaced. The adaptive load distribution shall be modified from the original load distribution using a procedure that considers the properties of the yielded structure.

Instead of using the uniform distribution to bind the solution, FEMA 356 also allows adaptive lateral load patterns to be used but it does not elaborate the procedure. Although adaptive procedure may yield results that are more consistent with the characteristics of the building under consideration it requires considerably more analysis effort. Fig. A.2 shows the common lateral load pattern used in pushover analysis.

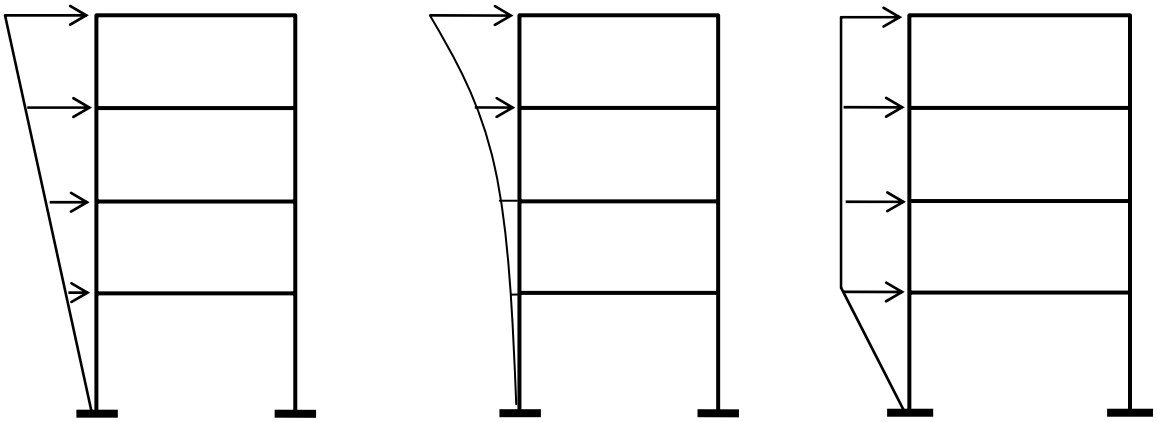

(a) Triangular (b) IS Code Based (c) Uniform

Fig. A.2: Lateral load pattern for pushover analysis as per FEMA 356 (Considering uniform mass distribution)

A.1.3 Target Displacement

Target displacement is the displacement demand for the building at the control node subjected to the ground motion under consideration. This is a very important parameter in pushover analysis because the global and component responses (forces and displacement) of the building at the target displacement are compared with the desired performance limit state to know the building performance. So the success of a pushover analysis largely depends on the accuracy of target displacement. There are two approaches to calculate target displacement:

(a) Displacement Coefficient Method (DCM) of FEMA 356 and

(b) Capacity Spectrum Method (CSM) of ATC 40.

Both of these approaches use pushover curve to calculate global displacement demand on the building from the response of an equivalent single-degree-of-freedom (SDOF) system. The only difference in these two methods is the technique used.

A.1.3.1 Displacement Coefficient Method (FEMA 356)

This method primarily estimates the elastic displacement of an equivalent SDOF system assuming initial linear properties and damping for the ground motion excitation under consideration. Then it estimates the total maximum inelastic displacement response for the building at roof by multiplying with a set of displacement coefficients.

The process begins with the base shear versus roof displacement curve (pushover curve) as shown in Fig. A.3a. An equivalent period (T_{eq}) is generated from initial period (T_i) by graphical procedure. This equivalent period represents the linear stiffness of the equivalent SDOF system. The peak elastic spectral displacement corresponding to this

period is calculated directly from the response spectrum representing the seismic ground motion under consideration (Fig. A.3b).

$$S_d = \frac{T_{eq}^2}{4\pi^2} S_a \qquad (A.1)$$

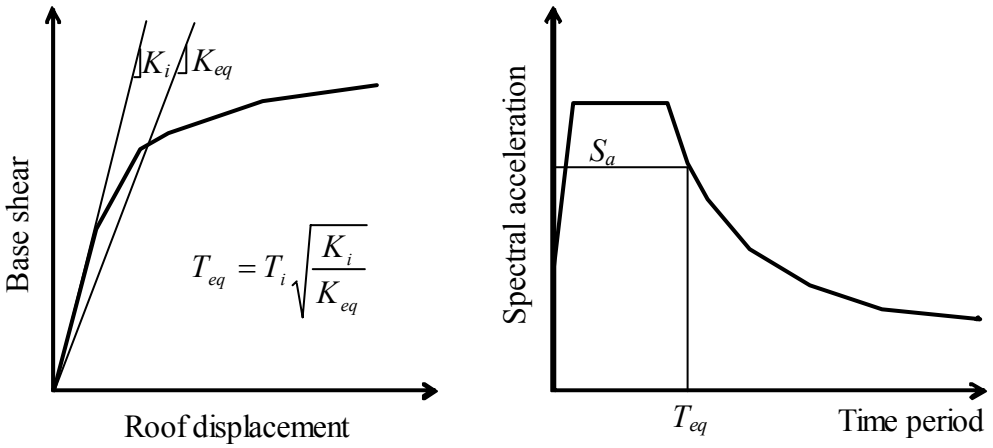

(a) Pushover Curve (b) Elastic Response Spectrum

Fig. A.3: Schematic representation of Displacement Coefficient Method (FEMA 356)

Now, the expected maximum roof displacement of the building (target displacement) under the selected seismic ground motion can be expressed as:

$$\delta_t = C_o C_1 C_2 C_3 S_d = C_o C_1 C_2 C_3 \frac{T_{eq}^2}{4\pi^2} S_a \qquad (A.2)$$

C_0 = a shape factor (often taken as the first mode participation factor) to convert the spectral displacement of equivalent SDOF system to the displacement at the roof of the building.

C_1 = the ratio of expected displacement (elastic plus inelastic) for an inelastic system to the displacement of a linear system.

C_2 = a factor that accounts for the effect of pinching in load deformation relationship due to strength and stiffness degradation

C_3 = a factor to adjust geometric nonlinearity (P-Δ) effects

These coefficients are derived empirically from statistical studies of the nonlinear response history analyses of SDOF systems of varying periods and strengths and given in FEMA 356.

A.1.3.2 Capacity Spectrum Method (ATC 40)

The basic assumption in Capacity Spectrum Method is also the same as the previous one. That is, the maximum inelastic deformation of a nonlinear SDOF system can be approximated from the maximum deformation of a linear elastic SDOF system with an equivalent period and damping. This procedure uses the estimates of ductility to calculate effective period and damping. This procedure uses the pushover curve in an acceleration-displacement response spectrum (ADRS) format. This can be obtained through simple conversion using the dynamic properties of the system. The pushover curve in an ADRS format is termed a 'capacity spectrum' for the structure. The seismic ground motion is represented by a response spectrum in the same ADRS format and it is termed as demand spectrum (Fig. A.4).

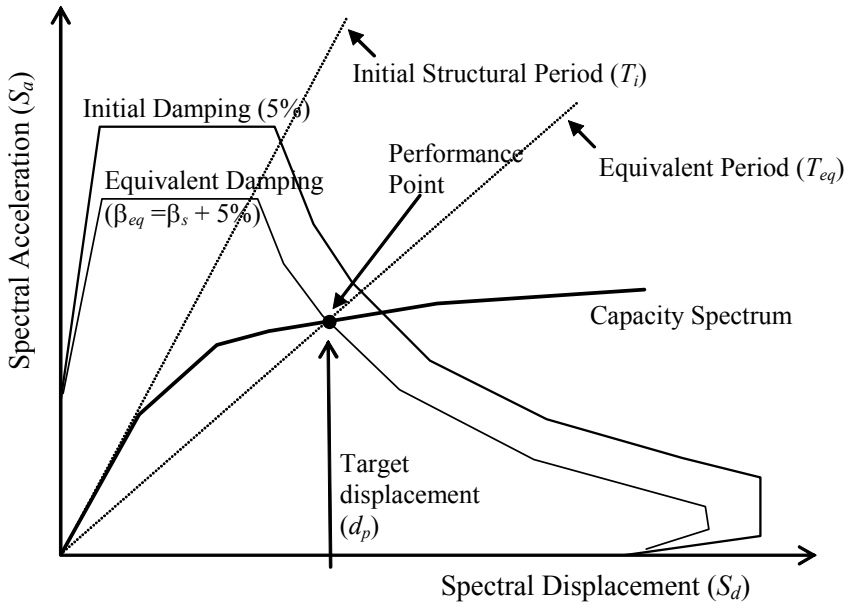

Fig. A.4: Schematic representation of Capacity Spectrum Method (ATC 40)

The equivalent period (T_{eq}) is computed from the initial period of vibration (T_i) of the nonlinear system and displacement ductility ratio (μ). Similarly, the equivalent damping ratio (β_{eq}) is computed from initial damping ratio (ATC 40 suggests an initial elastic viscous damping ratio of 0.05 for reinforced concrete building) and the displacement ductility ratio (μ). ATC 40 provides the following equations to calculate equivalent time period (T_{eq}) and equivalent damping (β_{eq}).

$$T_{eq} = T_i \sqrt{\frac{\mu}{1 + \alpha\mu - \alpha}} \qquad (A.3)$$

$$\beta_{eq} = \beta_i + k\frac{2(\mu - 1)(1 - \alpha)}{\pi\mu(1 + \alpha\mu - \alpha)} = 0.05 + \kappa\frac{2(\mu - 1)(1 - \alpha)}{\pi\mu(1 + \alpha\mu - \alpha)} \qquad (A.4)$$

Where α is the post-yield stiffness ratio and κ is an adjustment factor to approximately account for changes in hysteretic behavior in reinforced concrete structures.

ATC 40 relates effective damping to the hysteresis curve Fig. A.5 and proposes three hysteretic behavior types that alter the equivalent damping level. Type A hysteretic behavior is meant for new structures with reasonably full hysteretic loops, and the corresponding equivalent damping ratios take the maximum values. Type C hysteretic behavior represents severely degraded hysteretic loops, resulting in the smallest equivalent damping ratios. Type B hysteretic behavior is an intermediate hysteretic behavior between types A and C. The value of κ decreases for degrading systems (hysteretic behavior types B and C).

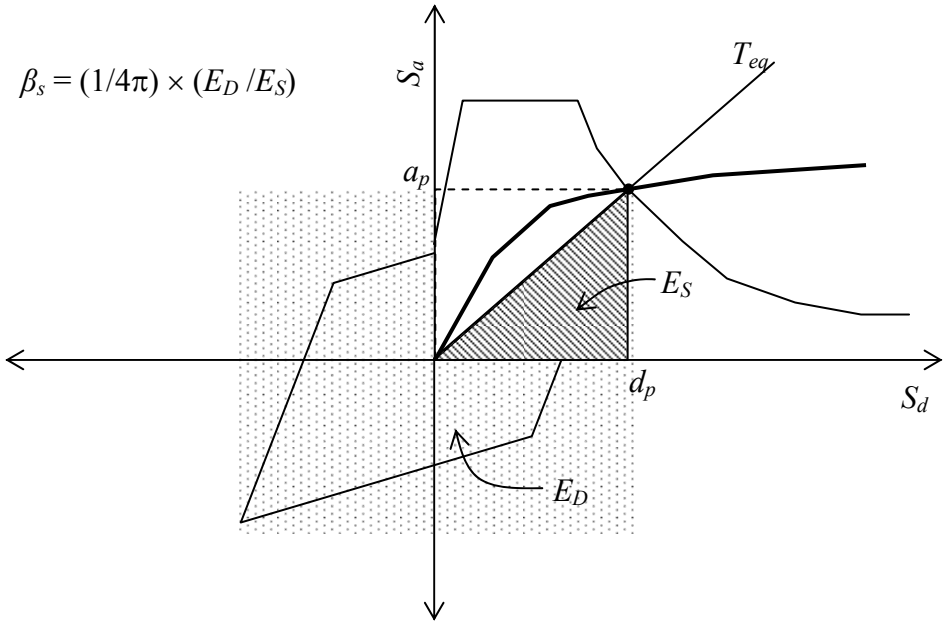

Fig. A.5: Effective damping in Capacity Spectrum Method (ATC 40)

The equivalent period in Eq. A.3 is based on a lateral stiffness of the equivalent system that is equal to the secant stiffness at the target displacement. This equation does not depend on the degrading characteristics of the hysteretic behavior of the system. It only

depends on the displacement ductility ratio (μ) and the post-yield stiffness ratio (α) of the inelastic system.

ATC 40 provides reduction factors to reduce spectral ordinates in the constant acceleration region and constant velocity region as a function of the effective damping ratio. The spectral reduction factors are given by:

$$SR_A = \frac{3.21 - 0.68ln(100\beta_{eq})}{2.2} \qquad (A.5)$$

$$SR_V = \frac{2.31 - 0.41ln(100\beta_{eq})}{1.65} \qquad (A.6)$$

Where SR_A is the spectral reduction factor to be applied to the constant acceleration region, and SR_V is the spectral reduction factor to be applied to the constant velocity region (descending branch) in the linear elastic spectrum.

Since the equivalent period and equivalent damping are both functions of the displacement ductility ratio (Eqs. A.3 and A.4), it is required to have prior knowledge of displacement ductility ratio. However, this is not known at the time of evaluating a structure. Therefore, iteration is required to determine target displacement. ATC 40 describes three iterative procedures with different merits and demerits to reach the solution.

REFERENCES

1. **A. Kadid and A. Boumrkik,** "Pushover analysis of reinforced concrete frame structures", Asian journal of civil engineering (building and housing) Vol. 9, No.1, pp. 75-83, 2008.

2. **A.Ghaffar, A.Javed, H.Rehman, K.Ahmed and M hyas,** "Development of shear capacity equations for rectangular reinforced beams", Park J Eng. & appl.Sci.Vol.6, pp.

3. **ACI 318,** Building Code Requirements for Reinforced Concrete, American Concrete Institute, Detroit, Michigan, 2002.

4. **Alexander Placas and Paul E. Regan and A.L.L Baker,** "Shear failure of reinforced concrete beams," ACI journal, title No.68-67, pp.763-773, October 1971.

5. **Applied Technology Council (ATC-40),** "Seismic evaluation and retrofit of concrete buildings", Vol.1& 2, California, 1996.

6. **ASCE-ACI Task Committee 426,** "The Shear Strength of Reinforced Concrete Members," ASCE Journal of Structural Div., Vol. 99, pp. 1091-1187, June 1973.

7. **Bazant Z P and Kazemi M T,** "Size effect on diagonal shear failure of beams without stirrups", ACI Structural Journal, 88(3), pp.268–276, 1991.

8. **Bazant Z P and Sun H H,** "Size effect in diagonal shear failure: influence of aggregate size and stirrups", ACI Materials Journal, 84(4) pp. 259–272, 1987.

9. **Bazant, Z. P., Yu and Qiang,** "Design Against Size Effect on Shear Strength of Reinforced Concrete Beams without Stirrups". Structural Engineering Report No.03-02/A466s, Northwestern University, Evanston, Illions, 2003.

10. **BS 8110-1, Structural use of concrete, Part 1:** Code of Practice for Design and Construction, British Standards Institution, London, 1997.

11. **C.G.Karayannis, C.E.Chalioris and P.D.Mavroeidis,** "Shear capacity of RC rectangular beam with continuous spiral transverse reinforcement", proceedings of Twelfth International Conference on Computational Methods and Experimental Measurements, Malta, pp.379-386, 2005.

12. **Chaitanya Patwardhan (2005),** "Shear strength and deformation modeling of reinforced Concrete columns", Department of Civil Engineering, Ohio State University, 2005.

13. **Chopra A.K and Goel R.K,** "A modal pushover analysis procedure to estimate seismic demands for buildings: Theory and preliminary evaluation", Report No PEER 2001/03, Pacific Earthquake Engineering Research Center, University of California, Berkeley, California, 2001.

14. **Comité Euro-International du Béton**, CEB-FIP Model Code 1990, Redwood Books, Wiltshire, England, pp.437, 1993.

15. **Dino Angelakos,** "The influence of concrete strength and longitudinal reinforcement ratio on the shear strength of large-size reinforced concrete bars with and without transverse reinforcement" Department of Civil Engineering, University of Toronto, 1999.

16. **F.F.Wafa, S.A.Ashour and G. S.Hasanian,** "Experiment investigations on shear behaviour of reinforced high strength concrete beam without shear reinforcement", Vol. 7, p.91-113, 1994.

17. **Federal Emergency Management Agency, FEMA-356**, "Pre standard and commentary for seismic rehabilitation of buildings". Washington (DC), 2000.

18. **G. Russo, G. Somma and P. Angeli,** "Design Shear Strength Formula for High Strength Concrete Beams", Journal of Material and Structures, 10(37), pp. 1519–1527, 2004.

19. **G.A.Rao and S.S.Injaganeri,** "Evaluation of size dependent design shear strength of reinforced concrete beams without web reinforcement", Sadhana Vol.36, Part 3, pp.393-410, 2011.

20. **Gastebled, Olivier J. and May Lan M,** "Fracture Mechanics Model Applied to Shear Failure of Reinforced Concrete Beams without Stirrups", ACI Structural Journal, pp.184-190, 1998.

21. **Gerin, M. and Adebar P.,** "Accounting for shear in seismic analysis of concrete structures", in Proceedings of the 13th World Conference on Earthquake Engineering, paper 1747. Vancouver, B.C., Canada, Aug. 2004.

22. **H.Sezen and E.J.Setzle,** "Model for the lateral behaviour of reinforced concrete columns including shear deformations earthquake spectra", Vol. 24, No. 2, pages 493–511, May 2008.

23. **IITM-SERC Manual,** Manual on seismic evaluations and retrofitting of RC building multi-storied RC building, March 2005.

24. **Indian Standard (IS 456),** "Plain and Reinforced Concrete – Code of Practice", 4^{th} revision, Civil Engineering Division Council, India, 2000.

25. **Kani G N J,** "The basic facts concerning shear failure", Proc. ACI Journal., 63(7), pp. 675–692, 1966.

26. **Kim J K and Park Y D,** "Shear strength of reinforced high strength concrete beams without web reinforcement, Magazine of Concrete Research, 46(166), pp. 7–16, 1994.

27. **Kim. W. and White R.N,** "Initiations of shear cracking in reinforced concrete beam with no web reinforcement." ACI structural journal, 88(3), pp.301-308, 1991.

28. **Kowalsky M.J., Priestley M.J.N., and Seible F.,** "Shear Behavior of Lightweight Concrete Columns Under Seismic Conditions," University of California, San Diego,Structural Systems Research Project, Report No. SSRP-95/10, pp.216, July 1995.

29. **Lynn, A. C., Moehle, J. P., Mahin, S. A., and Holmes, W. T.,** "Seismic evaluation of existing reinforced concrete building columns." Earthquake Spectra, 124_4_, pp. 715–739, 1996.

30. **M.Zakaria,T.Ueda, Z.Wu and L.Meng,** "Experimental investigations to clarify shear cracking behaviour of reinforced concrete beams with shear reinforcement", Journal of Advance Concrete Technology,Vol.7,No.1, pp.79-96, 2009.

31. **Marumaya M. and Jirsa J.O.,** " Shear Behavior of Reinforced Concrete Members under Bidirectional Reversed Lateral Loading, " CESRL Report No.78-1, University of Texas,Austin,1979.

32. **Mehmet Inel and Hayri Baytan Ozmen,** "Effects of plastic hinge properties in nonlinear analysis of reinforced concrete buildings", Department of Civil Engineering, Pamukkale University, 20070 Denizli, Turkey, 2006.

33. **Moehle J.P. and Mahin S.A.,** "Observations of the Behavior of Reinforced Concrete Buildings during Earthquakes," ACI SP-127, Earthquake-Resistant Concrete Structures Inelastic Response and Design, S.K. Ghosh, ed., American Concrete Institute, pp.67-89, 1991.

34. **Ousalem H., Kabeyasawa T.A., and Tasai Y.,** "Axial Load Collapse of Reinforced Concrete Columns Under Seismic Loading," 13th World Conference on Earthquake Engineering, pp.1233, Aug. 2004.

35. **P.Paczkowski and A.S.Nowak,** "Shear resistances of reinforced concrete beams without web reinforcements", Department of Civil Engineering, University of Nebraska, Lincoln, ne 68588-0531,USA,2008.

36. **Panagiotakos T.B. and Fardis M.N.,** "Deformations of Reinforced Concrete Members at Yielding and Ultimate," ACI Structural Journal, Vol. 98, 2, pp. 135-148, Mar-Apr., 2001.

37. **Priestley M.J.N., Verma R., and Xiao Y.,** "Seismic Shear Strength of Reinforced Concrete Columns," ASCE Journal of Structural Engineering, Vol. 120, pp. 2310-2329, Aug 1994.

38. **R. Park and T. Paulay,** "Reinforced Concrete Structures," Christ church, New Zealand, Aug, pp. 270-343, 1974.

39. **Roger Diaz de Cossio and Chester P. Siers,** "Behavior and Strength in Shear of beams and Frames without web reinforcement" ACI- Journal Feb., pp. 695-711, 1960.

40. **S. H Ahmad, A. R. Khallo, and A. Poveda,** "Shear Capacity of Reinforced High Strength Concrete Beams", ACI Structural Journal, 82(2), pp. 297–305,1986.

41. **S. Sarkar, O. Adwan, and B. Bose,** "Shear Stress Contribution and Failure Mechanisms of High Strength Concrete Beams", Material and Structures-RILEM, 32, pp. 112–116, 1999.

42. **S.Ahmad and A.Shah,** "Statistical model for the prediction of shear strength of high strength reinforced concrete beams" The Arabian Journal for Science and Engineering, Volume 34, Number 2B, 2009.

43. **S.Xu, H.W.Reinhardt and X.Zhang,** "Shear capability of reinforced concrete beams without stirrups predicted using a fracture mechanical approach", proceedings 11th International Conference on Fracture Turin, Italy, March 20-25, 2005.

44. **SAP 2000 (Version 11.0),** Integrated Software for Structural Analysis and Design. *Computers & Structures, Inc.*, Berkeley, California, 2007.

45. **Sezen H.,** "Seismic Behavior and Modeling of Reinforced Concrete Building Columns,"Ph.D. Dissertation, University of California, Berkeley, pp. 345, 2002.

46. **T.Chowdhury,** "Hysteretic modelling of shear-critical reinforced concrete columns" Thesis**,** The Ohio State University, 2007.

47. **T.J.Macginley and B.S.Choo,** "Reinforced concrete design theory and examples" second editions, pp.85-100, 1990.

48. **Theodore C. Zsutty.,** "Shear strength prediction for separate categories of simple beam tests" ACI journal, title No.68-15, pp. 138-143, Feb 1971.

49. **W. Chung and S.H. Ahmed,** "Model for shear critical High strength concrete beams," ACI Structural journal, title No.91-S4, Jan-Feb. pp. 31-41, 1994.

50. **Z. P. Bazant and J. K. Kim,** "The Size Effect in Shear Failure of Longitudinally Reinforced Beams", ACI Structure Journal, 81(5), pp. 456–468, 1984.

51. **Zsutty T C,** "Beam shear strength prediction by analysis of existing data, Proc. ACI J., 65(11), pp.943–951, 1968.